

**RELIABILITY-BASED FATIGUE DESIGN OF MARINE CURRENT TURBINE
ROTOR BLADES**

by

Shaun Hurley

A Thesis Submitted to the Faculty of
The College of Engineering and Computer Science
in Partial Fulfillment of the Requirements of the Degree of
Master of Science

Florida Atlantic University

Boca Raton, Florida

August 2011

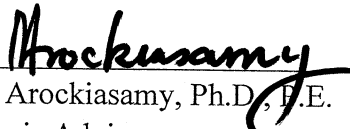
**RELIABILITY-BASED FATIGUE DESIGN OF MARINE CURRENT TURBINE
ROTOR BLADES**

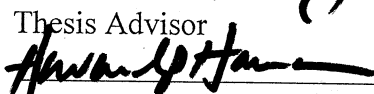
by

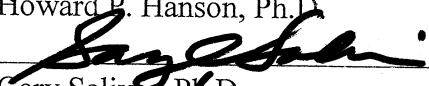
Shaun Hurley

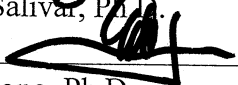
This thesis was prepared under the direction of the candidate's thesis advisor, Dr. Madasamy Arockiasamy, Department of Civil, Environmental and Geomatics Engineering, and has been approved by the members of his supervisory committee. It was submitted to the faculty of the College of Engineering and Computer Science and was accepted in partial fulfillment of the requirements for the degree of Master of Science.

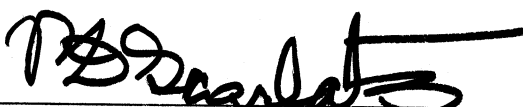
SUPERVISORY COMMITTEE:


M. Arockiasamy, Ph.D., P.E.
Thesis Advisor

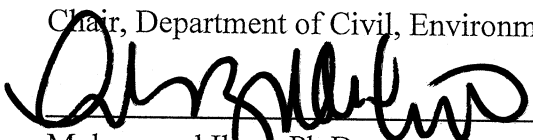

Howard B. Hanson, Ph.D.


Gary Salivar, Ph.D.

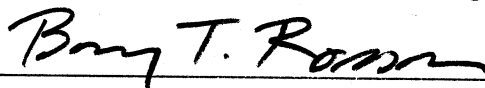

Yan Yong, Ph.D.


Panagiotis D. Scarlatos, Ph.D., P.E.

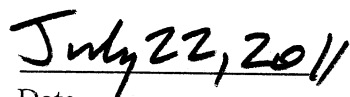
Chair, Department of Civil, Environmental and Geomatics Engineering


Mohammad Ilyas, Ph.D.

Interim Dean, College of Engineering and Computer Science


Barry T. Rosson, Ph.D.

Dean, Graduate College


Date

ACKNOWLEDGEMENTS

The work presented herein has been supported financially by the Southeast National Marine Renewable Center (SNMREC). This contribution is gratefully acknowledged. The author would like to thank Susan Skemp, Executive Director, and Dr. H.P. Hanson, Scientific Director for the constant encouragement.

The author wishes to express his sincere thanks to his thesis advisor Dr. M. Arockiasamy, Professor and Director, Center for Infrastructure and Constructed Facilities, Department of Civil, Environmental, and Geomatics Engineering, for his excellent guidance, suggestions, and constant review in all stages throughout the course of this work. Grateful acknowledgements are due to Dr. Gary Salivar and Dr. Yan Yong for being part my thesis committee. Their inputs and assistance were valuable in achieving the goals of the research. The author also expresses sincere appreciation to Dr. Knut Ronold at Det Norske Veritas for his constant feedback and suggestions throughout this study.

Finally, I am most grateful for the support, affection, and encouragement from my wife, parents, family and friends throughout the course of the research.

ABSTRACT

Author: Shaun Hurley

Title: Reliability-Based Fatigue Design of Marine Current Turbine Rotor Blades

Institution: Florida Atlantic University

Thesis Advisor: Dr. M. Arockiasamy, P.E.

Degree: Master of Science

Year: 2011

The study presents a reliability-based fatigue life prediction model for the ocean current turbine rotor blades. The numerically simulated bending moment ranges based on the measured current velocities off the Southeast coast line of Florida over a one month period are used to reflect the short-term distribution of the bending moment ranges for an idealized marine current turbine rotor blade. The 2-parameter Weibull distribution is used to fit the short-term distribution and then used to obtain the long-term distribution over the design life. The long-term distribution is then used to determine the number of cycles for any given bending moment range. The published laboratory test data in the form of an ε - N curve is used in conjunction with the long-term distribution of the bending moment ranges in the prediction of the fatigue failure of the rotor blade using Miner's rule. The first-order reliability method is used in order to determine the reliability index for a given

section modulus over a given design life. The results of reliability analysis are then used to calibrate the partial safety factors for load and resistance.

**RELIABILITY-BASED FATIGUE DESIGN OF MARINE CURRENT TURBINE
ROTOR BLADES**

LIST OF TABLES	ix
LIST OF FIGURES	x
CHAPTER 1 - INTRODUCTION.....	1
1.1 Introduction.....	1
1.2 Methodology and Approach	1
1.3 Objective and Scope	2
CHAPTER 2 – LITERATURE REVIEW	4
2.1 Introduction.....	4
2.2 Curve Fitting	5
2.3 Fatigue Life Prediction	7
2.4 Reliability Analysis	9
2.5 Partial Safety Factors	10
CHAPTER 3 – THEORY	12
3.1 Introduction.....	12
3.2 Rainflow Cycle Counting	12
3.3 MCT Rotor Blade Flapwise Bending Moment Loading History.....	17
3.4 Fatigue Strength and ε - N Curve	20
3.5 Damage Calculations	21
3.6 Reliability Analysis.....	22
3.7 Calibration of Partial Safety Factors.....	24
CHAPTER 4 – PROBABILISTIC AND DETERMINISTIC MODELING.....	26
4.1 Introduction.....	26
4.2 Loading History	27

4.2.1 Simulation modeling of full-scale rotor blades.....	27
4.2.2 Flapwise bending moment ranges at the rotor blade root	30
4.2.3 Turbulence intensity and mean current velocity	38
4.2.4 Two-parameter Weibull model	39
4.2.4.1 Cumulative probability of the bending moment range	39
4.2.4.2 Cumulative distribution function	41
4.2.4.3 Probability content	42
4.3 Fatigue Strength and ϵ -N Curve.....	48
4.3.1 Resistance and stiffness of composite laminates	48
4.3.2 Standard deviation of $\log K$ and m using the jackknife technique	52
4.3.3 Correlation coefficient	52
4.4 Fatigue Damage for MCT Rotor Blades	53
4.4.1 Miner's rule for cumulative damage.....	53
4.4.2 Damage calculations based on simulated bending moment ranges	54
4.4.3 Damage calculations based on the two-parameter Weibull model.....	54
4.4.4 Comparison of fatigue damage predictions	55
4.5 Effect of Non-Zero Mean Stress on Fatigue Damage.....	56
4.6 Model Uncertainty	58
4.6.1 Limit state function	58
4.6.2 Calibration of the scaling factor, k_r	58
CHAPTER 5 – RELIABILITY ANALYSIS.....	62
5.1 Introduction.....	62
5.2 Design Point and Z-value.....	63
5.3 Limit State Function	64
5.4 Reliability Index	67
CHAPTER 6 – CALIBRATION OF PARTIAL SAFETY FACTORS	71
6.1 Introduction.....	71

6.2 Characteristic ε - N Curve	71
6.3 Design ε - N Curve	72
6.4 Design Stress Range Distribution	74
6.5 Calibration of the Load Factor γ_f	75
CHAPTER 7 – SUMMARY, CONCLUSIONS, AND FUTURE WORK	78
7.1 Summary	78
7.2 Conclusions	79
7.3 Future Work	80
APPENDIX A Procedure	81
APPENDIX B Chapter 3 Codes	83
APPENDIX C Chapter 4 Codes	88
APPENDIX D Chapter 5 Codes	98
APPENDIX E Chapter 6 Codes	101
REFERENCES	102

LIST OF TABLES

Table 3.1 Rainflow Cycle Counting Results.....	17
Table 4.1 Calculation of Data Points for Cumulative Probability Plot.....	40
Table 4.2 Cumulative probabilities for BMR interval limits for one bin	43
Table 4.3 Number of cycles for Bin #6 containing 15,375 cycles.....	45
Table 4.4 Number of Exceeding Cycles in Design Life	46
Table 4.5 78 Pairs of $\log \varepsilon$ and $\log N$	49
Table 4.6 Bin # 6: Damage Calculations Using Simulated BMRs	54
Table 4.7 Bin # 6: Damage Calculations Using Weibull Model	55
Table 4.8 Compound BMR Damage Calculations	59
Table 4.9 Characteristic BMR Distribution Damage Calculations.....	60
Table 5.1 Summary of Mean and Standard Deviations of Stochastic Variables From Chapter 4.....	65
Table 5.2 Basic Stochastic Variables.....	66
Table 5.3 Compound BMR Damage Calculations Using the Design Point ε - N Curve....	66
Table 5.4 First-Order Reliability Method for $W = 0.007 \text{ m}^3$	69
Table 5.5 First-Order Reliability Method for $W = 0.0068 \text{ m}^3$	69
Table 5.6 First-Order Reliability Method for $W = 0.006905 \text{ m}^3$	70
Table 6.1 Damage Calculations Using Design SR Distribution and Design ε - N Curve.....	76

LIST OF FIGURES

Figure 3.1 A typical rainflow counting example	14
Figure 3.2 A typical rainflow counting using a computer program.....	15-16
Figure 4.1 The maximum, average, and minimum ocean current speed measured offshore Ft. Lauderdale, FL over a period of nearly 2 years	28
Figure 4.2 Significant wave height (ft) and peak wave direction for South FL	28
Figure 4.3 Peak wave period(s) and direction for South Florida.....	29
Figure 4.4 Coordinate system for the rotor blade of the marine current turbine	31
Figure 4.5 Out-of-plane bending moments for $u = 1.50$ m/s	32
Figure 4.6 Matlab results for out-of-plane bending moments for $u = 1.50$ m/s.....	33
Figure 4.7 30-minute time history for out-of-plane bending moments for $u = 1.50$ m	34
Figure 4.8 Comparison of bending moments for $u = 1.50$ & 1.51 m/s.....	35
Figure 4.9 Current velocities for the first 8-hour record.....	36
Figure 4.10 8-hour time history of bending moments for the first record	37
Figure 4.11 Cumulative distribution of simulated BMRs.....	40
Figure 4.12 Cumulative distribution function.....	42
Figure 4.13 Discretization of the cumulative distribution function for BMRs in a typical bin	44
Figure 4.14 Integration of BMR distributions over the design life.....	46
Figure 4.15 Strain amplitude versus number of cycles to failure	50
Figure 4.16 Least squares fit of ε - N data	51
Figure 4.17 Comparison of predicted cumulative damage	55
Figure 4.18 Characteristic BMR distribution.....	61
Figure 6.1 Characteristic ε - N curve	72
Figure 6.2 Design ε - N curve	74
Figure 6.3 Design BMR distribution	77

NOMENCLATURE

$D[]$	standard deviation	P_F	probability of failure
$E[]$	mean or expected value	R	radius of rotor blade
$\Phi ()$	standard normal cumulative distribution function	$[R]$	correlation matrix
*	design point	S	stress range (SR)
		S_{eq}	zero mean equivalent stress range
		S_m	mean stress range (SR)
		S_o	static strength of rotor blade
c	characteristic chord length	T_L	design life
C_L	lift coefficient	U_8	8-hour current velocity
D	damage	v_o	mean wave-current velocity at stalling
E	Young's modulus	w	reference wave-current velocity
e	residuals	W	section modulus
$F(x)$	cumulative probability	X	bending moment range (BMR)
$f(x)$	probability density	X^*	basic stochastic variable design point vector
F_M	random factor	X_a	adjustment BMR term
f_r	rotor blade frequency (per minute)	X_c	characteristic BMR
$g(x)$	limit state function	X_m	mean BMR
I_T	turbulence intensity	Z	Z-value
k_R	scale factor		
$\log K$	ε - N curve constant	β	reliability index
M	number of ε - N pairs	ε	strain range
m	ε - N curve constant	γ_f	load factor
N	number of cycles to failure	γ_m	material factor
n	number of exceeding cycles	ρ	correlation coefficient
N_r	number of rotor blade rotations in the design life	ρ_w	density of water

CHAPTER 1

INTRODUCTION

1.1 INTRODUCTION

The world is heavily dependent on fossil fuels which are not only on the verge of exhaustion, but are a cause of pollution and climate change. It is of interest to develop new and renewable energy systems. One such system is the development of marine current turbines.

Clean, power generation obtained through marine currents or tidal streams are becoming more popular. Studies indicate that marine currents have the potential to supply a large amount of future electricity needs. It has been estimated that capturing just 0.1% of the available energy from the Gulf Stream would supply Florida with 35% of its electricity needs. So far only a limited number of marine current energy devices have been installed in the US and Europe. One example is the twin rotor (HATT) system in Northern Ireland which supplies a maximum of 1.2MW of power (Senat, 2011).

1.2 METHODOLOGY AND APPROACH

Currently there is no well established method for the design of marine current turbine rotor blades, but the principals for design of wind turbine rotor blades, on the other hand, is relatively well established. The fundamental concepts for the design of

wind turbine rotor blades are adopted in the present study to examine the safety of marine current turbine (MCT) rotor blades against fatigue failure due to the flapwise bending moments based on site specific measured current velocity.

The safety of a marine current turbine (MCT) rotor blade against fatigue failure due to the computed flapwise bending moments based on site specific measured velocity is presented taking into account the inherent variability and statistical uncertainty in the load and resistance of the composite rotor blade. The load history is modeled on the basis of simulated bending moments using blade element momentum theory at the blade root of the rotor blade subjected to currents and the resistance is modeled in terms of an ε - N curve.

The present study also focuses on the reliability-based design of marine current turbine rotor blades. A comprehensive review is made of existing literature regarding fatigue life predictions, reliability analysis, and partial safety factors. The loading history and material strength are modeled and the statistical uncertainties of the modeling are taken into consideration in the reliability analysis. A reliability-based calibration of partial safety factors is performed for the rotor blade against fatigue failure in flapwise bending.

1.3 OBJECTIVE AND SCOPE

Chapter 2 reviews the available literature regarding curve fitting, fatigue life prediction, reliability analysis, and partial safety factors. The fundamental concepts of these topics are discussed and related to the present study.

Chapter 3 discusses the basic theory behind rainflow cycle counting, bending moment loading history, fatigue strength, damage calculations, reliability analysis, and

partial safety factors.

Chapter 4 illustrates the simulation of the loading history, modeling of the loading history, material characteristics, and Miner's rule for cumulative damage. A database of 8-hour simulated bending moment time histories is created for various current velocities using a numerical tool developed by Barltrop et al. (2006). The 8-hour bending moment time histories are rainflow counted and then placed in various bins based on their 8-hour mean current velocity and turbulence intensities. Each bin is fitted with a 2-parameter Weibull distribution. All of the bins are integrated and used in conjunction with Miner's rule and the ε - N curve to obtain the fatigue damage.

Chapter 5 covers the reliability analysis, specifically, the first-order reliability method and illustrates how the section modulus is related to the reliability. A limit state function is defined and the value of the section modulus that yields a limit state function of zero is iterated until a prescribed reliability index is reached.

Chapter 6 discusses the calibration of the partial safety factors. The material factor γ_m is calibrated to be the one that sets the design point ε - N curve (most probable ε - N curve) to the design ε - N curve. The load factor γ_f is calibrated to be the one that yields a cumulative fatigue damage exactly equal to one over the design life.

Finally, the summary, conclusions, and suggested future work are presented in **Chapter 7**.

CHAPTER 2

LITERATURE REVIEW

2.1 INTRODUCTION

While there is a great deal of literature containing information on wind turbine fatigue analysis, there is not nearly as much information on marine current turbine fatigue analysis. The procedure in the present study consists of reviewing the analysis of wind turbines, and then modifying the analysis for marine current turbines. The present study can be divided into four main sections including, curve fitting, calculation of fatigue damage, reliability analysis, and the calibration of partial safety factors.

The main objective in structural design calculations is the safety against failure (Braam et al, 1999). A computer program was developed for the probabilistic design of wind turbine rotor blades. The wind climate was represented in terms of generic long term distributions of 10-minutes mean wind speed and turbulence intensity. Based upon the wind climate, the short-term distributions of bending moment ranges were parameterized in terms of their first three statistical moments, including the mean, coefficient of variation, and skewness. The statistical moments of the bending moment range distributions were then characterized as functions of the 10-minute wind speed and turbulence intensity. The short term distributions were represented by a three-parameter

Weibull distribution. The short term distributions were integrated in order to obtain the long term distribution.

The fatigue properties of the rotor blade material were represented in terms of strain amplitude and number of cycles to failure. The cumulative fatigue damage was characterized by Miner's sum approach. Finally, a representation of model uncertainties associated with the various idealizations made was used in the estimation of the probability of fatigue failure in the design lifetime using the first-order reliability method.

2.2 CURVE FITTING

Manuel et al. (1999) continued the work that Winterstein et al. had presented in their 1994 study on fitting curves. The program used in this paper is known as the FITS routine. The program automatically fits a set of empirical data to a variety of distributions as well as computes the first four statistical moments of both the empirical data and the curves. The user inputs the empirical data points, selects the distribution desired, and the program generates the coefficients associated with the equation of the distribution. The concept is to generate the equation of a line that will best match the first four statistical moments of the empirical data.

The authors went through two examples: a wave height and a wind turbine load example. The wave height example had 19 data points, meaning 19 various wave heights. The data points were entered and the desired distributions were selected. The distributions used in that example were the Gumbel, shifted exponential above $H = 8\text{m}$, and shifted exponential above $H = 8.5\text{m}$. The program computes the first four statistical

moments of the actual data and of the three distributions selected. It was found that the Gumbel distribution overestimated the chances of larger wave heights.

The wind turbine example was slightly different in that it not only contained stress amplitude data points, but a corresponding number of occurrences with each stress range. The Weibull, quadratic Weibull, and cubic Weibull distributions were used in that example. The quadratic Weibull produced a much better fit than the standard Weibull distribution based on visual observation. The cubic Weibull distribution matched more statistical moments than the quadratic, but didn't turn out to be a significantly better fit. The cubic Weibull would be significantly better than the quadratic Weibull if the data displayed double curvature features. Overall, the quadratic Weibull distribution turned out to be the best pick to best represent the data when considering both computation time and the best fit.

Winterstein et al. (2001) published work on statistical moment-based fatigue load models for wind energy systems. Distributions of rainflow-counted range data were characterized by a limited number of statistical moments. In the study, several models were used that depended on these statistical moments. These models include a two-parameter Weibull model, quadratic Weibull model, and a damage-based model. The two-parameter model depends on the first two statistical moments while the quadratic model depends on the first three statistical moments. The damage-based model fits the first two statistical moments with a power-law transformation that directly reflects the damage. The damage-based model was found to be the best fit while the quadratic model gave a good fit as well, as long as the lower, non-damaging low-amplitudes were excluded.

Manuel et al. (2001) published literature on parametric models for estimating wind turbine fatigue loads for design. Statistical models were used to model data for in-plane and out-of-plane bending moments measured from a commercial wind turbine in a complex terrain. Ten-minute segments of bending moments are taken and rainflow-counted to obtain the bending moment ranges. The first three statistical moments were calculated for each ten minute segment. The non-damaging low-amplitude cycles were removed and quadratic Weibull distributions used to model the load distributions. The statistical moments were then expressed as a function of the wind speed and turbulence intensity in order to obtain the short-term distribution of bending moment ranges for any combination of wind speed and turbulence intensity. All of the short term distributions are then integrated to obtain the long-term distribution.

Ronold et al. (1999) published the results of the study on the reliability-based design of wind-turbine rotor blades. The procedure was similar to the previous procedures, but once the long-term distribution was obtained, another curve known as a characteristic curve was used to represent the data. The curve was not “fitted” in this case, but was based on a characteristic bending moment range distribution, which was a function of the properties of the wind-turbine.

2.3 FATIGUE LIFE PREDICTION

In the process of calibrating the partial safety factors for wind-turbine rotor blades, Ronold et al. (1999) carried out multiple cumulative fatigue damage calculations. A linear regression was used to model laboratory test results for strain ε versus number of cycles to failure N on a polyester laminate, yielding the ε - N curve. The empirical bending

moment range distributions (10-minute records) were sorted into bins and Miner's rule for cumulative damage was used in conjunction with the ε - N curve to predict the actual damage for each bin. Each bin was then modeled by a quadratic Weibull distribution, which was used to determine the number of cycles occurring for each bending moment range. Miner's rule was used to again predict the damage, but this time using the Weibull model distribution rather than the actual distribution. Each bin contained two damage predictions, one based on the actual bending moment range distribution and another based on the model distribution. The ratio between the two was calculated and the mean value of all of the bins was used as a factor applied to the damage caused by the Weibull distribution to account for any over or under prediction by the Weibull model.

Dowling's textbook on mechanical behavior of materials (2007) outlines several examples of fatigue life prediction ignoring and also including the effects of non-zero mean stresses. Given a stress amplitude that has a non-zero mean stress, Morrow's equation is used to calculate the equivalent stress amplitude that has a zero mean stress. This stress amplitude is used with the S - N curve to determine the number of cycles to failure. Miner's rule for cumulative damage is then used to calculate the damage. The inverse of the damage is finally used to predict the life. A typical example involved the life expectancy of 3,011 cycles being reduced to 781 cycles. This example shows the importance of considering the effect of non-zero mean stresses.

Hoskin et al. (1989) present statistical methods of Madsen et al. (1983) and Dirlik (1985) for prediction of fatigue damage rates and their applicability to wind turbine generator data. The paper discusses the development of the techniques to consider the

spectral characteristics of wind turbine rotor generator loads. The paper also presents a method for incorporating the low frequency component into the damage calculation.

Veers et al. (1998) reported a procedure for the analysis of measured loads to meet the needs of both fatigue life calculation and reliability estimates. The authors recommend that moments of the distribution of rainflow-range load amplitudes can be calculated and used to characterize the fatigue loading. These moments reflect successively the physical characteristics of the loading (mean, spread, tail behavior). Distributions of load amplitudes reflecting the damaging potential of the loadings are estimated from the moments at any wind condition of interest. Fatigue life is then calculated from the estimated load distributions.

2.4 RELIABILITY ANALYSIS

Young et al. (2010) carried out research on adaptive marine structures. One of the objectives of the research was to quantify the influence of material and operational uncertainties on the performance of self-adaptive marine rotors. The other objective was to develop a reliability-based design and optimization methodology for adaptive marine structures. A fluid-structure interaction model was used to generate the forces on the structure. The first-order reliability method was used to evaluate the influence of the uncertainties in the material and loading parameters. The first-order reliability method was used in order to optimize these design parameters. The results of the study reveal how it is more practical to use a reliability-based design rather than a deterministic approach for the design.

Low et al. (2002) developed a Microsoft Excel spreadsheet capable of performing a first-order reliability method. Although the study was focused on the design of a retaining wall, the procedure of the reliability analysis remains the same. The spreadsheet was set up with 5 columns, including the mean, standard deviation, design point, Z-value, and the correlation matrix. The design points were initially set equal to the mean values, but would be solved for later. One cell was set up that contained the formula for the limit state function. Another cell was set up that calculated the reliability index. The solver function was used to solve for the design points that yielded the smallest reliability index with a constraint of keeping the limit state function equal to zero. The results of the reliability analysis were found to agree and closely with the results of a Monte Carlo simulation using 500,000 trials.

Ronold et al. (1999) used the first-order reliability method in order to determine the reliability of damage predicted by the models. As the variables for the models were calculated, the mean and standard deviations were calculated as well. The first-order reliability method was carried out by calibrating the section modulus until the resulting reliability index was equal to the desired reliability index. The design points are the most likely values of the variables at failure.

2.5 PARTIAL SAFETY FACTORS

Ronold et al. (1999) used the results of the first-order reliability method in order to calibrate the partial safety factors. The characteristic bending moment range distribution as described in section 2.2 was used in order to represent the characteristic

long-term bending moment range distribution over the design life of 20 years. The curve was used to determine the number of cycles occurring at a given bending moment range.

The characteristic ε - N curve was then obtained by shifting the fitted ε - N curve to the left by two standard deviations of the residuals. This is a standard procedure for ε - N curves that yields a 95% confidence level. The design point ε - N curve was calibrated during the first-order reliability method but the damage was based on the expected values that were originally calculated. The ideal design ε - N curve (characteristic ε - N curve with an applied material factor) is the one that matches the design point ε - N curve. The material factor was calculated so as to set the design ε - N curve to the design point ε - N curve. The sought-after choice for the load factor is the one that will lead to a cumulative damage exactly equal to one by using the design load distribution (characteristic load distribution with an applied load factor) and design ε - N curve. The material factor was calculated to be 1.150 and the load factor to be 1.088.

Toft et al (2010) has shown the calibration of partial safety factors for fatigue design of wind turbine blades. The stochastic models for the physical uncertainties of the material properties are based on constant amplitude fatigue tests. The uncertainty in the Miner's rule for linear damage accumulation is determined from variable amplitude fatigue tests. The partial safety factors are calibrated for different variations of the stochastic models. The load and resistance factors were calculated to be 1.00 and 1.37, respectively.

CHAPTER 3

THEORY FOR MARINE CURRENT TURBINE (MCT) FATIGUE LOADS CONSIDERING STATISTICAL VARIATION AND RELIABILITY-BASED CALIBRATION OF PARTIAL SAFETY FACTORS

3.1 INTRODUCTION

This chapter presents a brief summary of the basic concepts and the theory related to the statistical variation associated with the fatigue loads of the rotor blade of a marine current turbine. The rainflow cycle counting method, flapwise bending moment time histories at the root of the rotor blade, fatigue strength and ε - N curve, fatigue damage calculations using Miner's rule and reliability analysis are discussed for the calibration of partial safety factors. The concepts adopted in the present study are similar to the published research for representation of wind induced bending moment ranges (BMRs) in wind turbine rotor blades (Ronold et. al, 1999).

3.2 RAINFLOW CYCLE COUNTING

Counting methods have been developed for the study of fatigue damage generated in structures. Various counting methods include level crossing, peak, simple range, and rainflow. The rainflow cycle counting method, which is the preferred method, has initially been proposed by M. Matsuiski and T. Endo to count the half cycles of strain-

time signals (Lalanne et. al, 1999). The rainflow method was developed in order to count irregular cycles.

The rainflow cycle counting method is utilized in order to count the load cycles. There are two main ways to count the number of cycles for a given set of data points, which can be accomplished manually, or by a computer. Both techniques involve initially rearranging the data, if necessary. The rainflow cycle counting always begins with an extreme value, either the largest or smallest. Any data before that extreme value is shifted to the end of the data.

When rainflow counting manually, the first step is to plot the points, connect them and turn the graph sideways. The lines connecting the points can be thought of as roofs of a house. Assuming the largest value is chosen as the starting point, a theoretical 'raindrop' is placed and observed to see where it flows. The rain drop will flow just as a real raindrop would flow on the roof of a house. There are two conditions that will terminate the flow of the raindrop. As the raindrop falls off of an edge (valley, in this case) and there are no more lines (roofs) directly below for the raindrop to fall on to, the rainflow stops. The second condition that will terminate the rainflow is if it runs into a previous rainflow path. The order that the rainflow paths are to be evaluated is from the largest to smallest peaks. The y-values of each cycle are found from the beginning and end of each cycle. The mean and range can be calculated from the y-values.

An example is shown below in Figure 3.1. The highest peak starts at 80 and the rainflow path does not terminate until -100, giving a range of 180. The next highest peak is 80 as well, and that rainflow path continues until -40, yielding a range of 120. The third highest peak is 60, which continues to 20, giving a range of 40. This procedure is

continued until all peaks have been accounted for. Always excluding the final peak, there are 6 peaks in this example, and therefore, 6 ranges (cycles).

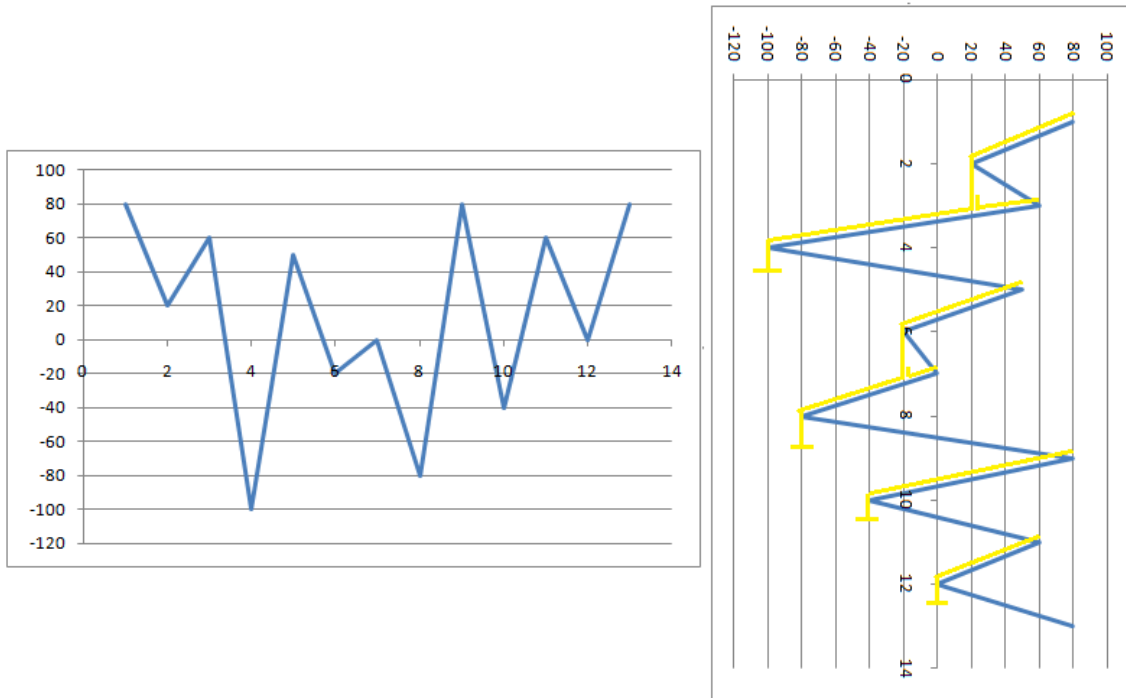


Figure 3.1 – A typical manual rainflow counting example

The computer program used in the present study was coded using MATLAB (Appendix B). The first step in this computer program is to calculate all of the ranges. The program analyzes the data from the beginning to the end, and searches for a range that is less than or equal to the range immediately following it. When the computer program locates this range, the two data points that make up this range are stored into a matrix, and then deleted from the data set. There are now two less data points, resulting in one less range in the data set. The program will start from the beginning again and continue this process until there is no more data. An example of the rainflow counting technique is illustrated below by modeling each step of the process. Each range

represents half of a cycle (Figure 3.2). The 2nd range, 40 (Figure 3.2(a)) is less than the 3rd range, 160, so the points that make up the 2nd range (20 and 60) are deleted as shown in Figure 3.2(b). The graph is redrawn as shown in Figure 3.2(c). This procedure is repeated until there are only three points left as shown in Figure 3.2(j).

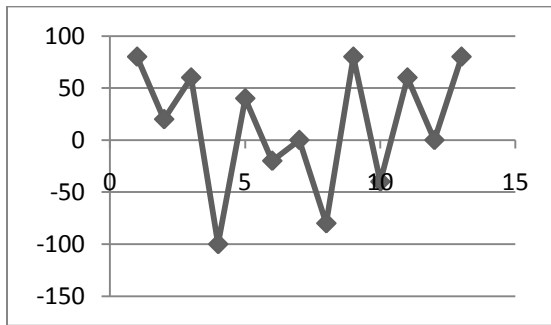


Figure 3.2 (a)

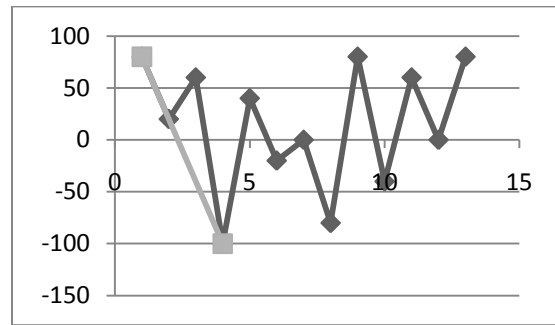


Figure 3.2 (b)

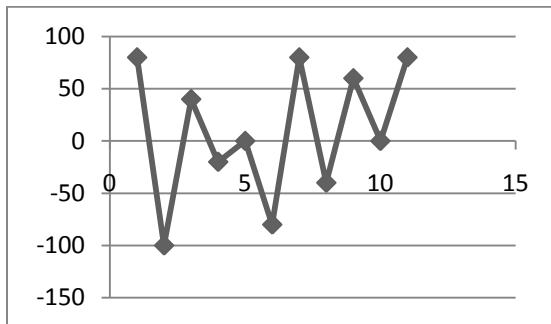


Figure 3.2 (c)

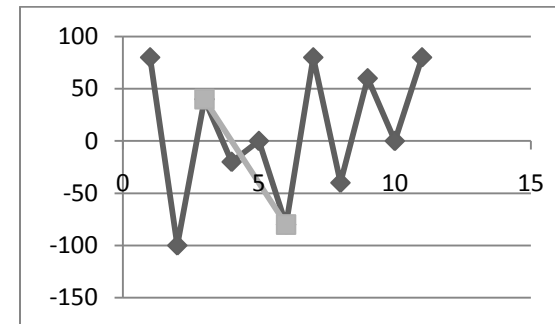


Figure 3.2 (d)

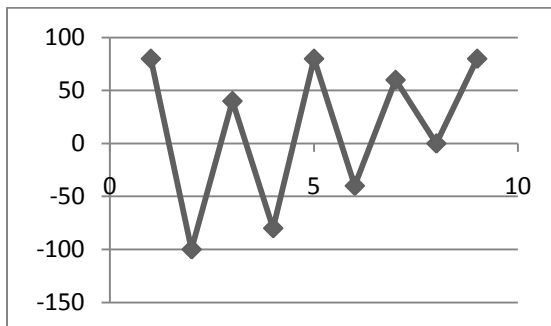


Figure 3.2 (e)

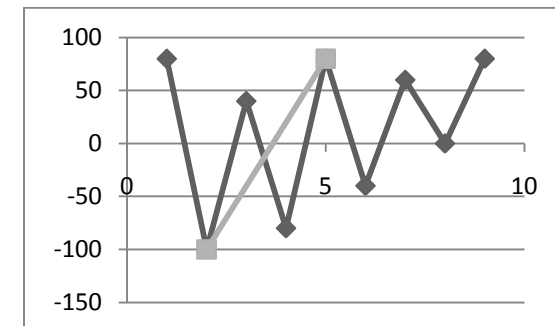
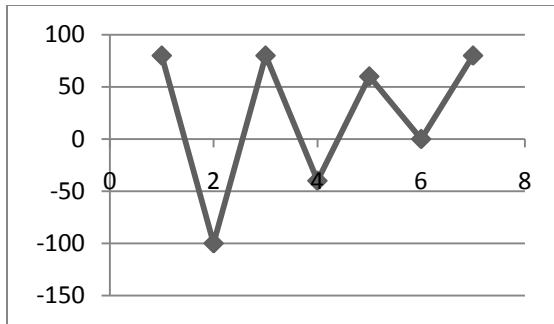


Figure 3.2 (f)



(1st two points are deleted)

Figure 3.2 (g)

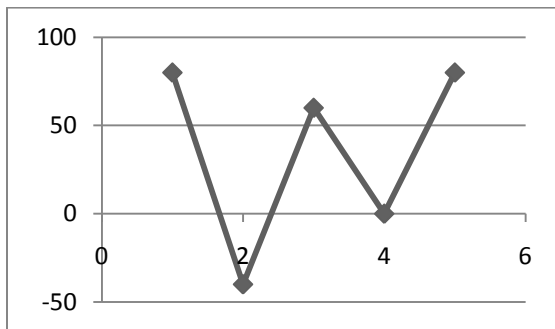


Figure 3.2 (h)

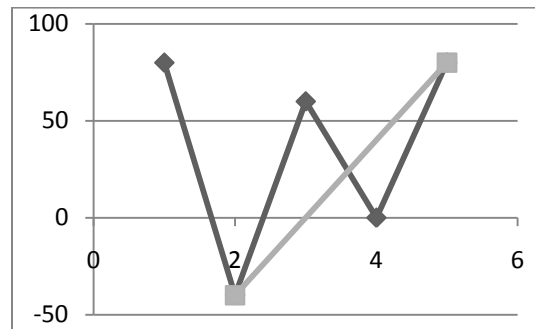


Figure 3.2 (i)

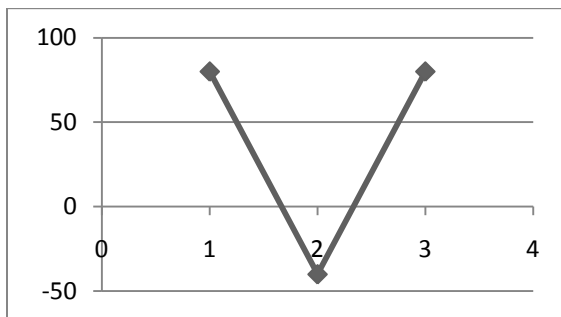


Figure 3.2 (j)

Figure 3.2(a-j) – A typical example of rainflow counting using a computer program

To summarize, below is a table of the ranges that were counted along with their associated mean values.

Table 3.1 – Rainflow Cycle Counting Results

Cycle #	Deleted After Figure #	Range	Mean
1	3.1	40	40
2	3.3	20	-10
3	3.5	130	-15
4	3.7	180	-10
5	3.8	60	30
6	3.10	120	20

3.3 MCT ROTOR BLADE FLAPWISE BENDING MOMENT LOADING HISTORY

Bending moment time histories are generated based on the blade element-momentum theory combined with linear wave theory. The calculations are made using the numerical tool developed by Barltrop et al. (2006). For every wave current velocity, a unique bending moment time history is generated that covers a 30-minute period.

A total of one month's worth of wave current velocities are used in the calculations, which is divided into 8-hour intervals. Each 8-hour interval contains 16 various current velocities and therefore, 16 bending moment time histories that are arranged in succession. The mean wave current velocity $E[U_8]$ and turbulence intensity I_T are calculated within each 8-hour interval. I_T is calculated using Equation 3.3-1.

$$I_T = \frac{D[U_8]}{E[U_8]} \quad (3.3-1)$$

where $D[U_8]$ is the standard deviation of the velocities. Also, for each 8-hour interval, the rainflow counting technique is used in order to count the BMRs X , where each BMR represents one load cycle.

Based upon the variation of mean current velocities and turbulence intensities, bins are created. Each bin is defined by a range of mean current velocities and range of

turbulence intensities. Based upon each 8-hour interval's mean current velocity and turbulence intensity, the BMRs associated with the interval are sorted into their respective bins.

In a given bin, the BMRs are arranged in ascending order. The cumulative probability of each BMR is calculated by method of median ranks given by

$$F(x_i) = \frac{n_i - 0.3}{n + 0.4} \quad (3.3-2)$$

where $F(x_i)$ represents the cumulative probability of a given BMR X that occurs n_i times and n is the total number of BMRs in the bin. A 2-parameter Weibull model is used to model the cumulative probability distribution for each bin. The probability density function for the Weibull distribution is given as

$$f(x) = ba^{-b}x^{(b-1)}\exp\left(-\left(\frac{x}{a}\right)^b\right) \quad (3.3-3)$$

where the constants a and b are determined so as to fit the BMRs contained within each bin using Matlab's curve fitting program. After the determination of the constants a and b , the integral of the density function (cumulative distribution function (CDF) – Equation 3.3-4) is used to determine the probability content. The CDF is given by

$$F(x) = 1 - \exp\left(-\left(\frac{x}{a}\right)^b\right) \quad (3.3-4)$$

The probability content is probability of a given BMR occurring in a given interval. This is done by discretizing the distribution into several intervals, calculating the cumulative probability of both ends of a given interval, and taking the difference of the cumulative probabilities. The total number of load cycles in the entire bin is multiplied by the probability content of each interval in order to obtain the number of cycles that are

expected to occur within a given interval of BMRs. The total number of cycles within each interval is assumed to occur at the mean BMR value of the interval. This process is repeated for every bin to obtain pairs of BMRs X and number of cycles n .

Once pairs of X and n are obtained from every bin, they are integrated to generate the load distribution, or load spectrum. A characteristic load distribution is then fit to best represent the data pairs of X and n as shown in Equation 3.3-5

$$X = X_a + k_R X_c \left(1 - \frac{\log(n)}{\log(3N_r)} \right) \quad (3.3-5)$$

where n represents the number of exceeding cycles, N_r is the number of rotor blade fatigue cycles in the design life T_L , X_a is the adjustment BMR value, k_R is a scaling factor, and X_c is the characteristic bending moment. The characteristic bending moment X_c is defined by the Danish code (Dansk Ingeniørforening, 1992) and shown below

$$X_c = \frac{\rho_w}{2} w^2 c C_L \frac{R^2}{3} \quad (3.3-6)$$

where ρ_w is the density of water, R is the radius of the rotor blade, C_L is the lift coefficient, c is the characteristic chord length, and w is the reference wave-current velocity. The radius of the rotor blade R is taken as the distance from the center of the hub to the tip of the blade and is equal to 10 meters. The lift coefficient C_L and characteristic chord length c are both taken at a distance of $2R/3$ from the center of the hub. The reference current velocity w is assumed to be given by

$$w^2 = \left(\frac{4\pi}{3} f_r R \right)^2 + v_o^2 \quad (3.3-7)$$

where v_o is the mean wave-current velocity at stalling and f_r is the number of rotations per minute.

3.4 FATIGUE STRENGTH AND ε - N CURVE

Published data are available on pairs of strain amplitude ε and number of cycles to failure N based on laboratory test results. Based on the scatter plot of ε - N pairs, a linear regression is performed in order to obtain a best fit line, known as an ε - N curve. The equation for this ε - N curve is given by

$$\log N = E[\log K] - E[m]\log \varepsilon + E[e] \quad (3.4-1)$$

where $\log K$ and m are coefficients, e represents the residuals, and $E[]$ represents the mean value. The residuals are simply the horizontal distances from each ε - N pair to the ε - N curve.

The mean and standard deviation of the residuals are also calculated using the formulae shown below

$$E[e] = \frac{1}{M} \sum_{i=1}^M e_i \quad (3.4-2)$$

$$D[e] = \sqrt{\frac{1}{M-1} \sum_{i=1}^M (e_i - E[e])^2} \quad (3.4-3)$$

where $D[]$ represents the standard deviation and M represents the total number of ε - N pairs. Due to the nature of the liner regression, the mean value for e is virtually zero, and is known as the zero-mean term.

Since the results of the least squares regression yield only one value for $\log K$ and one value for m , these values are taken to represent the mean values. A resampling technique must be used to obtain the standard deviations as well as the correlation coefficient between $\log K$ and m . In this paper, the jackknife technique is used.

The jackknife technique involves removing one pair of ε and N at a time and recalculating the coefficients $\log K$ and m . For example, the first pair of ε and N is removed and the coefficients $\log K$ and m are calculated by performing the linear regression. The first pair of ε and N is then placed back into the data set and the second pair of ε and N is removed. The coefficients $\log K$ and m are recalculated, and this process is repeated until every pair of ε and N has been removed at one point. This results in several values of $\log K$ and m . The standard deviations are then calculated by using Equations 3.4-4 and 3.4-5 shown below.

$$D[\log K] = \sqrt{\frac{M-1}{M} \sum_{i=1}^M ((\log(K))_i - E[\log(K)])^2} \quad (3.4-4)$$

$$D[m] = \sqrt{\frac{M-1}{M} \sum_{i=1}^M (m_i - E[m])^2} \quad (3.4-5)$$

The correlation coefficient is calculated using Equation 3.4-6.

$$\rho = \frac{\frac{M-1}{M} \sum_{i=1}^M [(\log(K))_i - E[\log(K)]] * [m_i - E[m]]}{D(\log K) * D[m]} \quad (3.4-6)$$

3.5 DAMAGE CALCULATIONS

Within each bin, two damage calculations are made based on Miner's rule for cumulative damage: one based on the simulated bending moment loading history and another based on the fitted 2-parameter Weibull distribution. Miner's rule is given by

$$D = \sum_{i=1} \frac{\Delta n(S_i)}{N(S_i)} \quad (3.5-1)$$

where Δn represents the number of stress cycles occurring at a given stress range S_i and N represents the number of cycles to failure for the same stress range S_i as determined from the ε - N curve.

In order calculate the damage, the BMR is first converted to the stress range by dividing by the section modulus W as shown in Equation 3.5-2.

$$S = \frac{X}{W} \quad (3.5-2)$$

The stress range can then be related to the strain amplitude which yields the number of cycles to failure. The stress range is given as Equation 3.5-3.

$$S = 2E\varepsilon \quad (3.5-3)$$

Within each bin, the damage based on the actual loading history is calculated by using the results of the rainflow counting technique. The damage based on the 2-parameter Weibull distribution is also calculated for each bin.

Within each bin, a random factor F_M is calculated as the ratio of the damage based on the simulated loading history and the damage based on the 2-parameter Weibull distribution (Equation 3.5-4).

$$F_M = \frac{\text{damage predicted by simulated BMRs}}{\text{damage predicted by Weibull model}} \quad (3.5-4)$$

The mean and standard deviation of the random factor are calculated. These are calculated to account for any over or under prediction of the model and used in the reliability analysis.

3.6 RELIABILITY ANALYSIS

The limit state function $g(x)$ is defined as one minus the random factor times the

damage calculated from the design point ε - N curve and empirical BMRs. This can be seen below in Equation 3.6-1

$$g(x) = 1 - F_M^* D(\mathbf{X}^*) \quad (3.6-1)$$

where \mathbf{X}^* is a vector containing the design points of the stochastic variables.

There are several basic stochastic variables that are used in the calculation of the limit state function. The design points of these variables are defined as the most likely values at time of failure and are denoted with an asterisk*. Failure occurs when the limit state function become less than or equal to zero. The Z-value (found on the standard normal cumulative distribution table (Ayyub et al., 1997)) for each variable is calculated using Equation 3.6-2

$$Z = \frac{\mathbf{X}^* - E[\mathbf{X}]}{D[\mathbf{X}]} \quad (3.6-2)$$

where $E[\mathbf{X}]$ and $D[\mathbf{X}]$ are the mean and standard deviation vectors of the variables (Ayyub et al., 1997). To start with, these design points are unknown and the results of the reliability analysis will give these values. A correlation matrix $[\mathbf{R}]$ including all basic stochastic variables is also constructed to account for any correlations that exist between the variables. A section modulus is selected and a first-order reliability analysis is carried out as described in Low et al. (2002).

The concept of the reliability analysis is to solve for the design points that not only yield a limit state $g(x)$ of zero, but that also yield the smallest reliability index β given by Equation 3.6-3.

$$\beta = \min \sqrt{\left[\frac{\mathbf{X}^* - E[\mathbf{X}]}{D[\mathbf{X}]} \right]^T [\mathbf{R}]^{-1} \left[\frac{\mathbf{X}^* - E[\mathbf{X}]}{D[\mathbf{X}]} \right]} \quad (3.6-3)$$

Constraining the design point values to the values that yield the smallest reliability index gives the most probable combination of design point values that yield a limit state of zero. In other words, the smallest reliability index is associated with the most likely values for the variables at failure. The section modulus is changed until the resulting reliability index β matches the desired reliability index.

3.7 CALIBRATION OF PARTIAL SAFETY FACTORS

It is standard procedure to select the characteristic ε - N curve as the curve that is shifted to the left by a factor of two times the standard deviation of the residuals $D[e]$ (Ronold et al., 1999). The characteristic ε - N curve is defined by Equation 3.7-1.

$$\log N = E[\log K] - E[m] \log \varepsilon - 2D[e] \quad (3.7-1)$$

A pair of partial safety factors, including a material factor γ_m and load factor γ_f is applied to the characteristic ε - N curve and the characteristic load distribution, respectively. This gives the design ε - N curve (Equation 3.7-2)

$$\log N = E[\log K] - E[m] \log(\gamma_m \varepsilon) - 2D[e] \quad (3.7-2)$$

and the design load distribution (Equation 3.7-3).

$$X = \gamma_f \left(X_a + k_R X_c \left(1 - \frac{\log(n)}{\log(3N_r)} \right) \right) \quad (3.7-3)$$

Since the reliability index was calculated using the design point values, the desired material factor is one that will yield the design point ε - N curve equal to the design ε - N curve. The design point ε - N curve and design ε - N curve are set equal to each other to solve for the material factor.

Once the material factor is calculated, the damage over the design life is calculated using the design ε - N curve and the design load distribution. The load factor is calibrated to be the one that leads to a damage exactly equal to one.

CHAPTER 4

PROBABILISTIC AND DETERMINISTIC MODELING

4.1 INTRODUCTION

A marine current turbine (MCT) with 20 meter diameter rotor blades is considered in this study. The hypothetical full scale marine current turbine has a rotor with a fixed rotational speed $f_r = 7$ rpm and positioned at 40 meters depth below the mean sea level. The rotor blade is assumed to be made up of a polyester laminate reinforced by five layers of combined woven glass roving and chopped strand mat with fibers oriented at 0/90. The Young's modulus E for the polyester laminate with reinforcements is taken as 29.7×10^9 Pa. The design life T_L of the rotor blade is assumed to be 20 years.

Published literature on wave-current interactions in marine current turbines shows that the out of plane bending moment at the root of the rotor blade is approximately four times the in-plane bending moment at the root (Barltrop et al., 2006). In this paper, the bending moment at the root of the rotor blade is assumed to fluctuate with significant amplitudes. The Southeast National Marine Renewable Center has made measurements of the current velocities over a two year period off the Southeast coast line of Florida. This paper uses the marine current velocities extending over a period of one month. The wave current velocities were measured at 30-minute intervals for a period of one month. Nearly two years of measurements were taken and the mean current speed near the

surface is nearly 1.7 m/s and can exceed 1.0 m/s at depths of up to 150 meters. On an average, the Florida Current decreases monotonically with depth to a weak 0.19 m/s near the ocean bottom at 320 m, on the outer edge of the Miami Terrace. In the top 100 meters, the current speed ranges between 1.0 and 2.0 m/s 85% of the time. At 50 and 100 m depths, the flow exceeded 2.0 m/s only 3.3% and 0.06% of the time, respectively.

Flapwise bending moment ranges (BMR) at the rotor blade root, and load sequence effects are variables that can be considered to have uncertainties. These variables are used in the reliability analysis, specifically, the first-order reliability method (Chapter 5). In order to perform the first-order reliability method, the mean value, standard deviation, and correlation coefficient of any uncertainties need to be calculated. Throughout this thesis, the mean $E[]$, standard deviation $D[]$, and if applicable ρ , the correlation coefficient between any variables are calculated.

4.2 LOADING HISTORY

4.2.1 Simulation modeling of full-scale rotor blades

The measured current velocities near the core of Florida current offshore are used in the evaluation of the loads on the full-scale rotor blades (Figure 4.1).

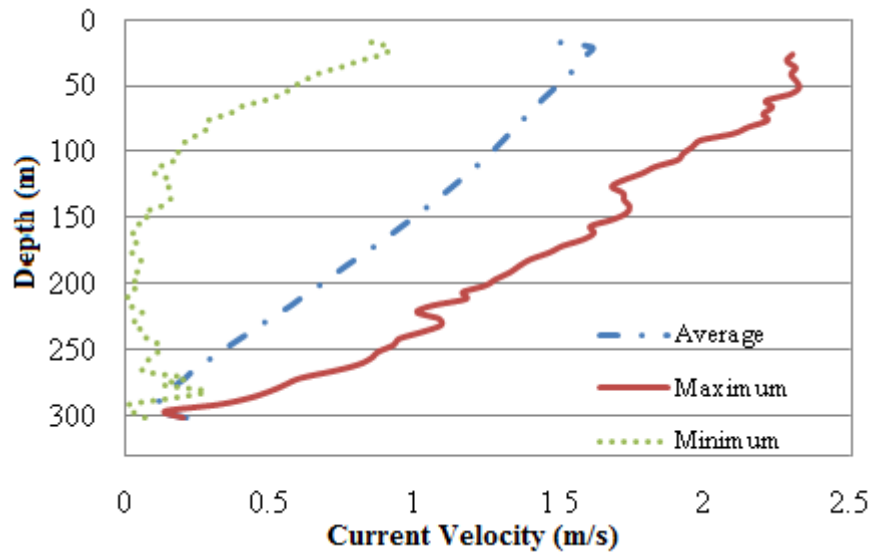


Figure 4.1 - The maximum, average, and minimum ocean current speed measured offshore Ft. Lauderdale, FL over a period of nearly 2 years. Velocity measurements were made at 30-minute intervals with a 75 kHz ADCP.

Figures 4.2 and 4.3 show the experimental South Florida Gulfstream and Wave Forecasts using the Simulating Waves Nearshore (SWAN) wave model and the Real Time Ocean Forecast System.

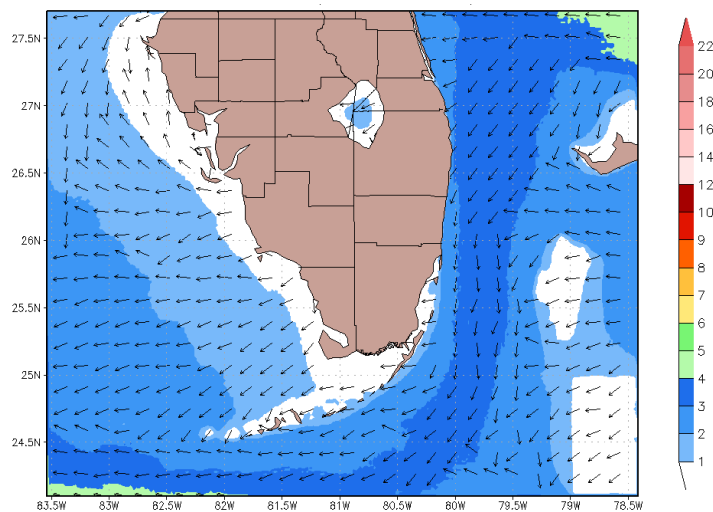


Figure 4.2 - Significant wave height (ft) and peak wave direction for South Florida (source: NOAA, WFO MIA SWAN forecast)

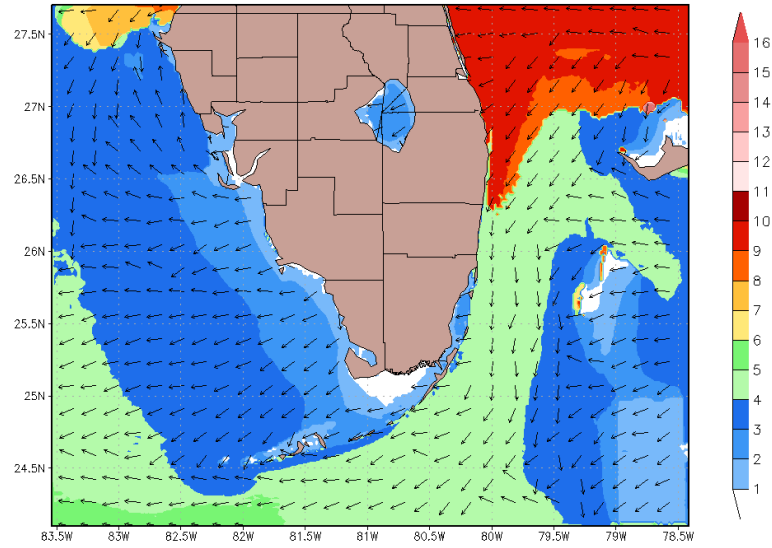


Figure 4.3 - Peak wave period(s) and direction for South Florida (Source: NOAA, WFO MIA SWAN forecast)

Since the available power generation levels are directly related to the marine current velocity, it is essential to describe statistically the marine current velocity distributions. The description of the current characteristics will yield the energy content of the currents on a given site and their energy distribution. The energy content determines whether it is worthwhile installing a turbine on any given site and the energy distribution provides information about the prevalent current speeds to help with the turbine design. In the present study numerical simulations are carried out using a mathematical model to generate the hydrodynamic forces and bending moments on the 20 m diameter tri-bladed horizontal-axis turbine.

The model rotor has essentially a wind turbine configuration with a slight increase in blade chord and thickness for structural strength. The rotor uses three blades and has a diameter of 20 meters. The blades merge into the hub without taper and its angles can be adjusted over a range of limited degrees. The blade section used in the study follows the

section S814 developed by Somers (1997). The S814 is one of the series created by the NREL, USA for wind turbines. One important characteristic of the S814 is the minimal sensitivity of its maximum lift coefficient to roughness effects, which is a critical property for stall-regulated wind turbines. The aerofoil has a very low drag coefficient and is also not too sensitive to change of angle of attack around the stalling angle. In general, the aerofoil profile for the blade is chosen based on its good performance at low Reynolds number and its tolerance to surface imperfections (Barltrop et al., 2006).

In the simulation model, numerical calculations are carried out for every time step on the assumption of quasi-steady flow. The rotor parameters are defined based on the pitch angle, coning angle, hub radius, and root radius. Interpolation functions are defined for twist angle and chord length along the blade length. The torque, thrust and bending moments induced by the stream flow are calculated using MathCAD. Lift and drag coefficients are determined as function of incident angles taking into account the 3D effects. Limited parametric studies are carried out to better understand the influence of important parameters on the performance of the rotor. Simulated thrust and torque are obtained when rotor operates in calm water and waves. The variation in the thrust and torque is predicted for certain parameters including wave height and wave frequency. The thrust and torque are evaluated by varying both the rotor's rotational speed and current speed (Senat, 2011 and Senet et al., 2011).

4.2.2 Flapwise bending moment ranges at the rotor blade root

The flapwise (out-of-plane) bending moment histories are generated (Figure 4.4) based on the blade element-momentum theory combined with the linear wave theory.

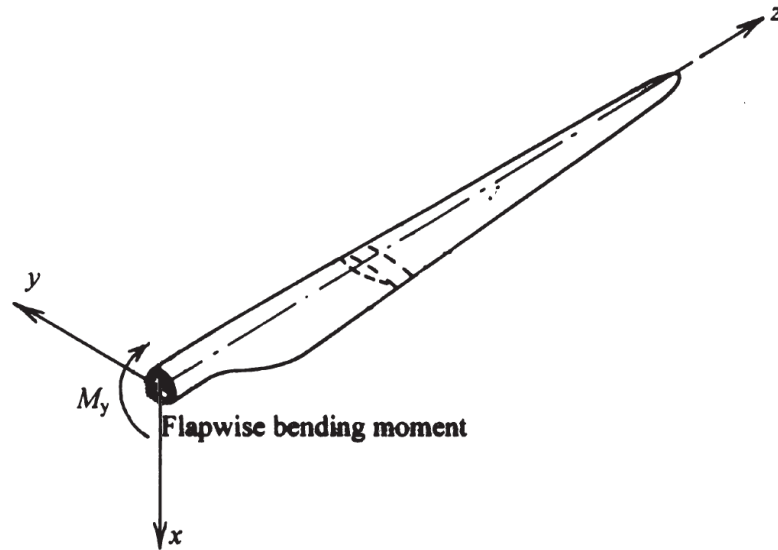


Figure 4.4 – Coordinate system for the rotor blade of the marine current turbine

The bending moments are computed using the numerical tool developed by Barltop et al. (2006). The computation of bending moments is based on 20 meter rotor blades of a full-scale marine current turbine with a fixed rotational speed of 7 rpm at a water depth of 40 meters below the mean sea level. The approximate range of the current velocities measured over a typical one month period was 1.50 m/s to 2.0 m/s. A typical out-of-plane bending moment time history is shown below in Figure 4.5 (Hurley et al., 2011).

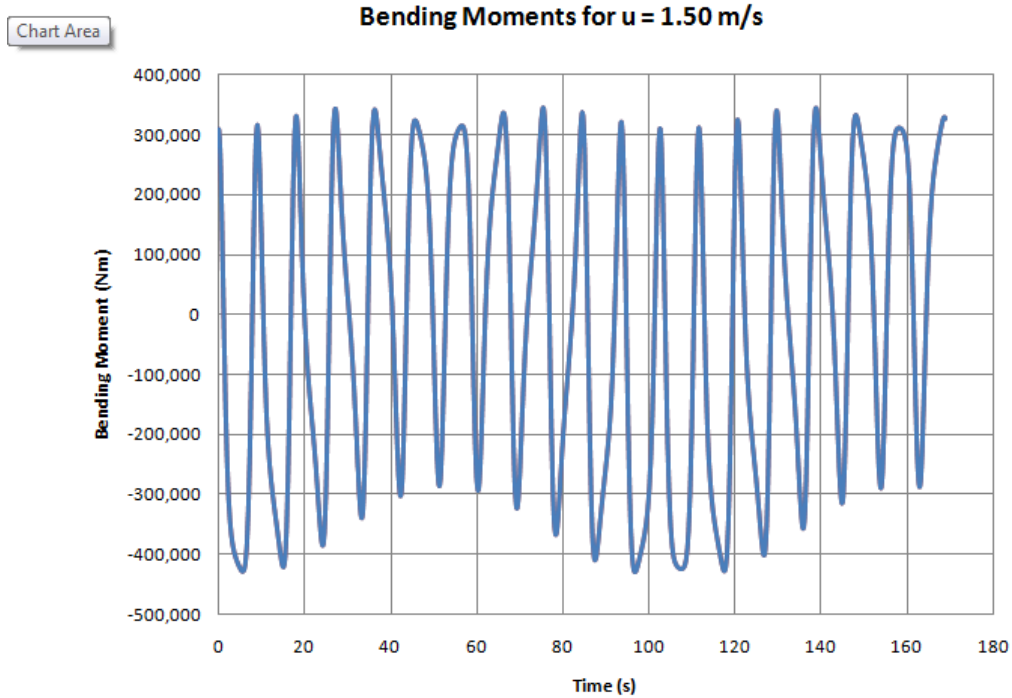


Figure 4.5 – Out-of-plane bending moments for $u = 1.50$ m/s

This figure shows only the computed bending moments over a representative period of the first 170 seconds in a typical time period of 30 minutes. It can be observed from Figure 4.5 that the bending moment time history for a current velocity of 1.50 m/s approximately repeats about every 96.8 seconds. For different current velocities, this period changes slightly. The recorded data indicates mean current velocities ranging from 1.50 m/s to 2.03 m/s. The computed time histories of bending moments for different current velocities showed a similar pattern in the bending moment variation over time.

The time at which the time history repeats itself is considered in the determination of the number of repetitions needed to simulate the data over a 30-minute duration. For example, the BMRs are obtained for a current velocity of 1.50 m/s over a 30 minute

(1800 seconds) duration by repeating the data $1800/96.8 = 18.6$ times.

The out-of-plane bending moment histories are computed at a time step of 0.07 second intervals. In the present study the rainflow counting technique is chosen for illustration of the methodology, although the bending moments simulated from the numerical model in the present study are not quite random. The variations in bending moment time histories are quantified using the rainflow counting method based on the peaks and valleys. A special purpose Matlab program (Appendix B) is written to extract the peaks and valleys from the bending moment time histories. Figure 4.6 shows only the peaks and valleys for one typical repetition of the bending moment time history corresponding to a current velocity of 1.50 m/s (the first 96.8 second duration).

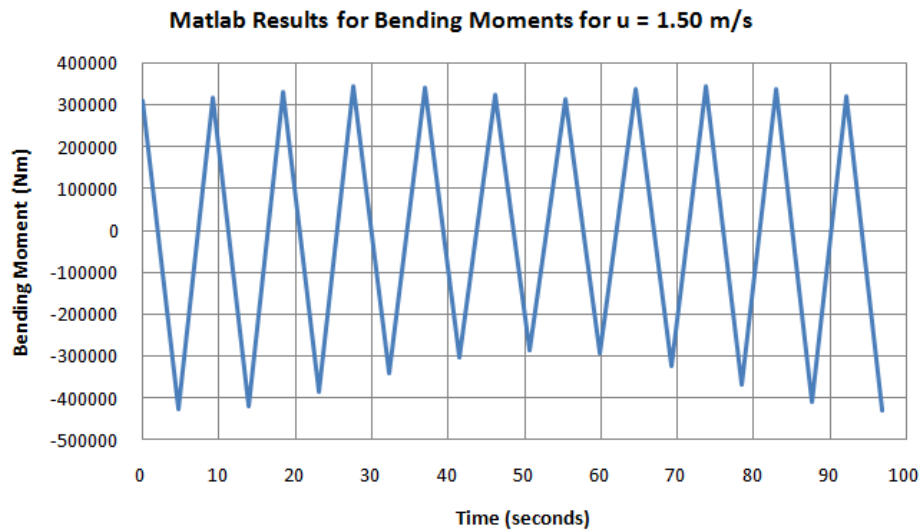


Figure 4.6 - Matlab results for out-of-plane bending moments for $u = 1.50$ m/s

The bending moment history shown in Figure 4.6 is repeated 18.6 times to obtain the full bending moment time history over a 30 minute duration as shown in Figure 4.7. The first 96.8 seconds (Figure 4.6) can be seen in the dotted box.

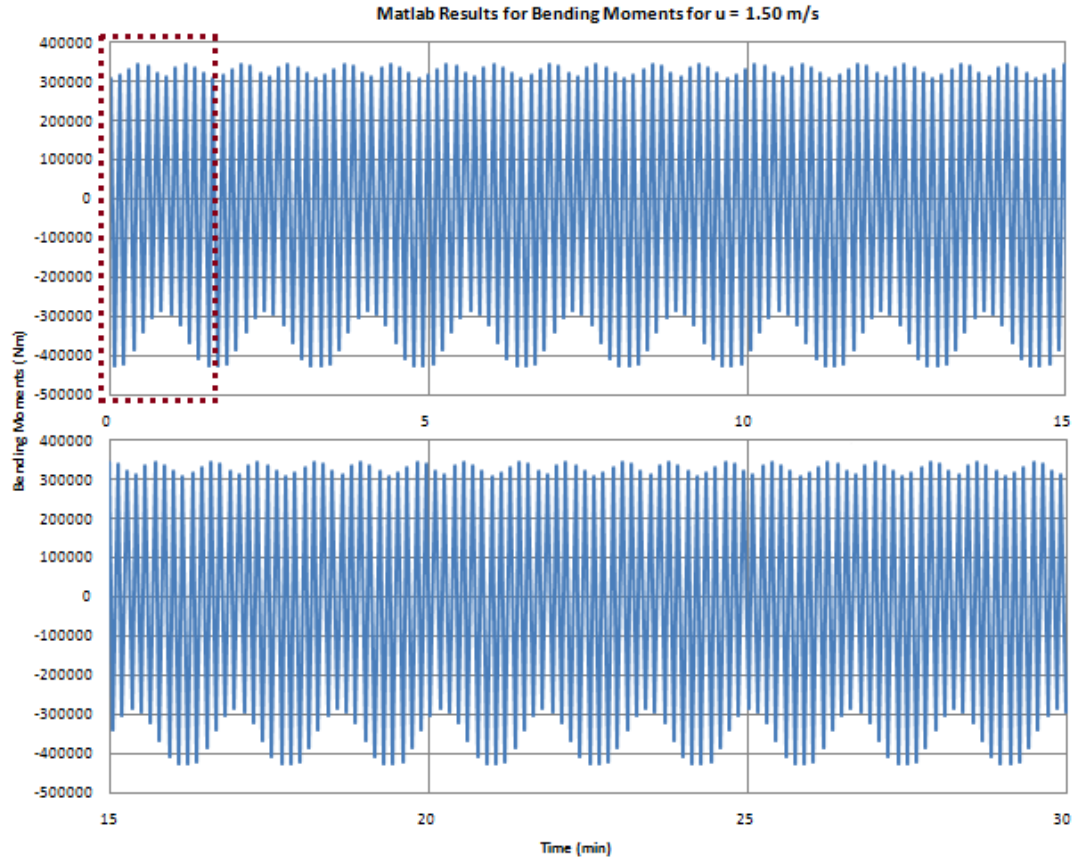
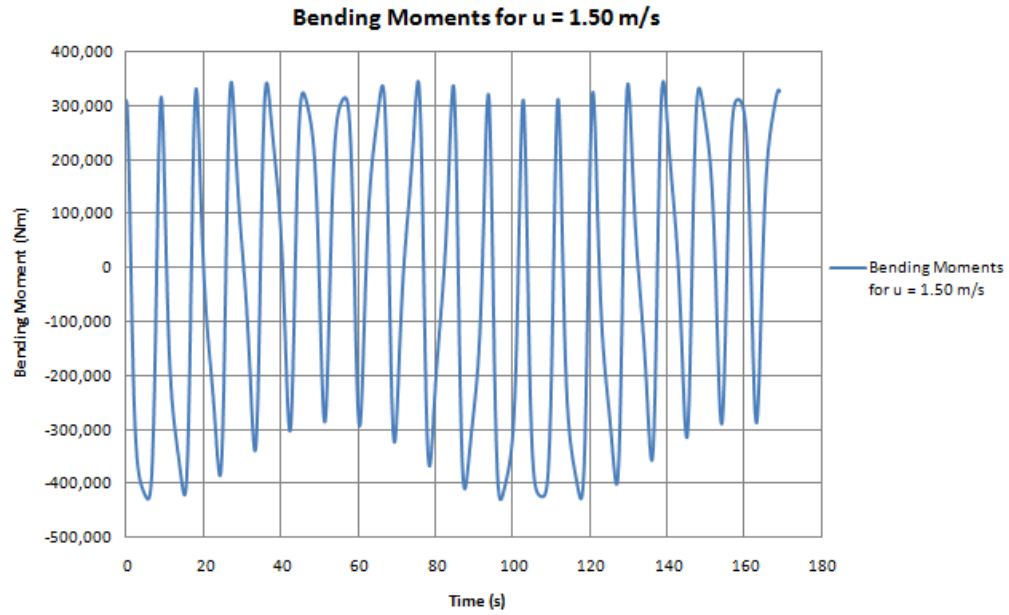
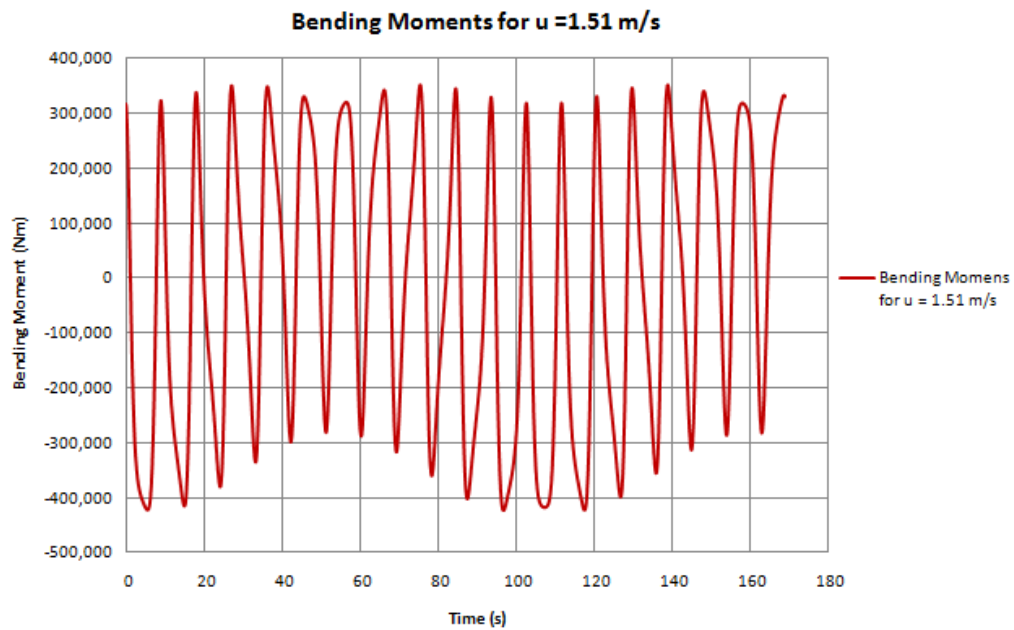


Figure 4.7 – 30-minute time history for out-of-plane bending moments for $u = 1.50$ m/s

The available recorded velocity data over a typical one month period is chosen for illustration. A database is generated for bending moment time histories by repeating the above procedure for varying mean current velocities ranging from 1.50 – 2.03 m/s at increments of 0.01 m/s. This data shows the largest observed current velocity to be 2.03 m/s. Although the observed velocities were recorded to the nearest thousandth of a meter per second, they are rounded to the nearest hundredth m/s to save computational time and effort. The first 170 seconds of the bending moment time histories for current velocities of 1.50 m/s and 1.51 m/s are compared and shown in Figure 4.8.



(a)



(b)

Figures 4.8 (a) and (b) – Comparison of bending moments for $u = 1.50$ and 1.51 m/s

The bending moment time histories shown in Figure 4.8 do not exhibit any significant

difference in the magnitudes due to a difference in the current velocities of 0.01 m/s. Therefore, rounding off the current velocity from the thousandth m/s to the nearest hundredth m/s was reasonable in the numerical simulation.

An 8-hour record consists of 16 measured discrete velocities recorded at 30-minute intervals. The bending moment time histories for a typical 8-hour record are generated based on the database already established for current velocities from 1.50 m/s to 2.03 m/s. As an example, the first 8-hour record in the one month period under consideration consisted of the following velocities: 1.57, 1.67, 1.70, 1.65, 1.67, 1.68, 1.66, 1.72, 1.75, 1.66, 1.73, 1.73, 1.79, 1.83, 1.78, and 1.72 m/s shown in Figure 4.9.

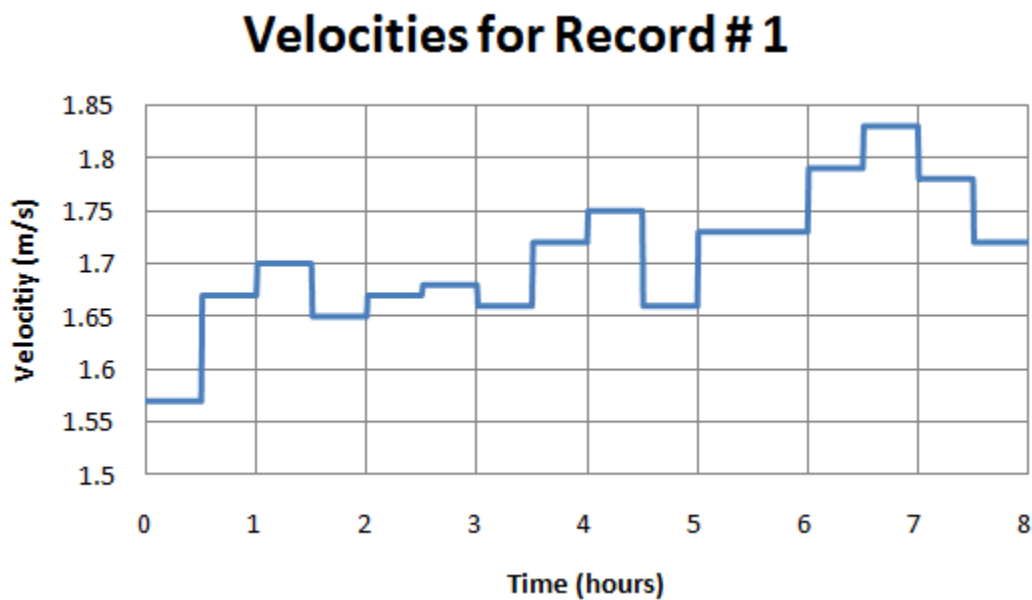


Figure 4.9 - Current velocities for the first 8-hour record

A unique bending moment time history is associated with each current velocity and the time histories are arranged in succession to obtain the bending moment time history for

the entire 8-hour record. As an example, the full bending moment time history is shown in Figure 4.10 for one of the 8-hour records.

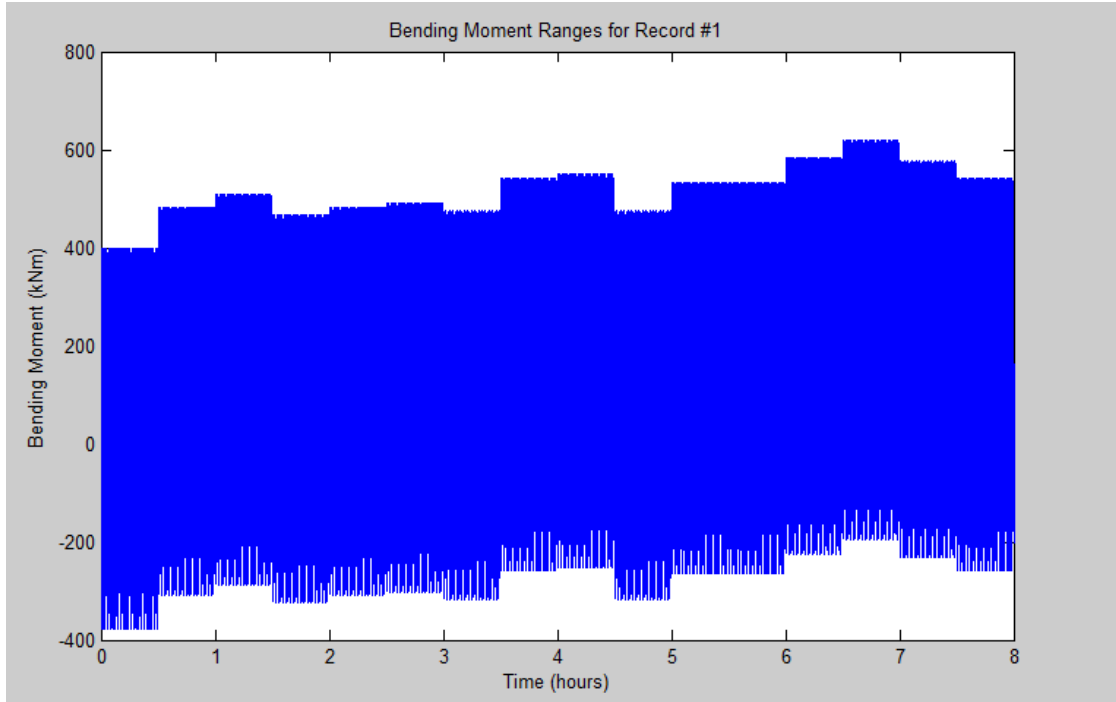


Figure 4.10 – 8-hour time history of bending moments for the first record

The effect of non-zero mean stresses is generally ignored in the analysis of cumulative fatigue damage. The present study considers the influence of mean stress in the fatigue life prediction (Section 4.5). For each 8-hour record, the average mean bending moment is computed from the time histories. The average and standard deviations of the mean bending moments for all 8-hour records for the chosen one month period are calculated to be

$$E[X_m] = 119,339 \text{ N-m}; \quad D[X_m] = 82,573$$

These values are later used in the reliability analysis in Chapter 5.

4.2.3 Turbulence intensity and mean current velocity

Bins are created in the study based on different values of mean current velocities, $E[U_{8-hour}]$ and turbulence intensities, I_T for each 8-hour record. The turbulence intensity is calculated using Equation 3.3-1 shown below

$$I_T = \frac{D[U_8]}{E[U_8]} \quad (3.3-1)$$

where $D[U_8]$ is the standard deviation of the velocities. These bins are created in order to place similar bending moment time histories together to arrive at an optimal Weibull fit. The mean velocity and turbulence intensity for the first 8-hour record are computed to be 1.71 m/s and 0.037, respectively. This procedure is repeated for each 8-hour record in the one month period. Typically, any one month period consists of ninety 8-hour records. The rotor blades are assumed to stall at velocities smaller than 1.50 m/s and hence, the simulation was carried out for only velocities greater than or equal to 1.50 m/s.

A total of 11 bins are created, each with a bin width of 0.1 m/s for the mean current velocities and 0.05 for the turbulence intensities. The limits on the bin widths based on the mean current velocities and turbulence intensities range from 1.50 m/s to 2.00 m/s and 0 to 0.15, respectively.

Up to this point, the mean velocity $E[U_8]$, turbulence intensity I_T , and BMRs are determined for each 8-hour record. The BMRs from all 8-hour records are placed into the respective bins based on the 8-hour mean current velocity and turbulence intensity. Each bin now contains BMRs from multiple 8-hour records for the one month period. In order to fit the BMRs to a cumulative distribution function (Section 4.2.4), the magnitude of the BMRs in each bin are first arranged in ascending order.

4.2.4 Two-parameter Weibull model

The Weibull distribution is a continuous probability density function and is commonly used to model material strength. The Weibull distribution interpolates between the exponential distribution and Rayleigh distribution, both of which are special types of the Weibull distribution. The exponential distribution is obtained by setting the shape factor equal to one, and is used to describe events that occur continuously at a constant average rate. The Rayleigh distribution is obtained by setting the shape factor equal to two, and is used to describe events that contain two-dimensional vectors that are normally distributed, uncorrelated, and have equal variance. Due to the nature of wave and currents, the Weibull distribution, which can handle the complexities of both the exponential distribution and Rayleigh distribution, is a good selection. In the present study, the Weibull model is used to model the cumulative probability of the BMRs for each bin.

4.2.4.1 Cumulative probability of the bending moment range

The Weibull distribution is normally plotted on probability paper where the x-axis and y-axis represent $\ln(X)$ and $\ln(-\ln(1-F(x)))$, respectively, where X represents the BMR and $F(x)$ represents the cumulative probability. The cumulative probability of the simulated BMRs is calculated using median ranks

$$F(x_i) = \frac{n_i - 0.3}{n + 0.4} \quad (3.3-2)$$

where $F(x_i)$ is the cumulative probability of a given BMR X occurring. In other words, there are n_i occurrences of a given BMR or less than that given BMR out of the total

number of bending moments ranges n , in the bin. A plot of the cumulative probability of the BMRs in a typical bin is created using Table 4.1 and is plotted in Figure 4.11. It can be seen from Table 4.1 in the fourth column that there are a total of 15,345 occurrences, therefore $n = 15,345$.

Table 4.1 – Calculation of Data Points for Cumulative Probability Pot (Appendix C)

BMR X (N-m)	$\ln(X)$	Number of Occurrences	Cumulative Number of Occurrences, n_i	Cumulative Probability $F(x_i)$	$\ln(-\ln(1-F(x_i)))$
499,000	13.12	1	1	4.56E-05	-10.00
507,000	13.14	1	2	1.11E-04	-9.11
581,000	13.27	1	3	1.76E-04	-8.65
.
.
.
802,000	13.59	47	15282	9.96E-01	1.70
804,000	13.60	31	15313	9.98E-01	1.82
805,000	13.60	32	15345	1.00E+00	2.30

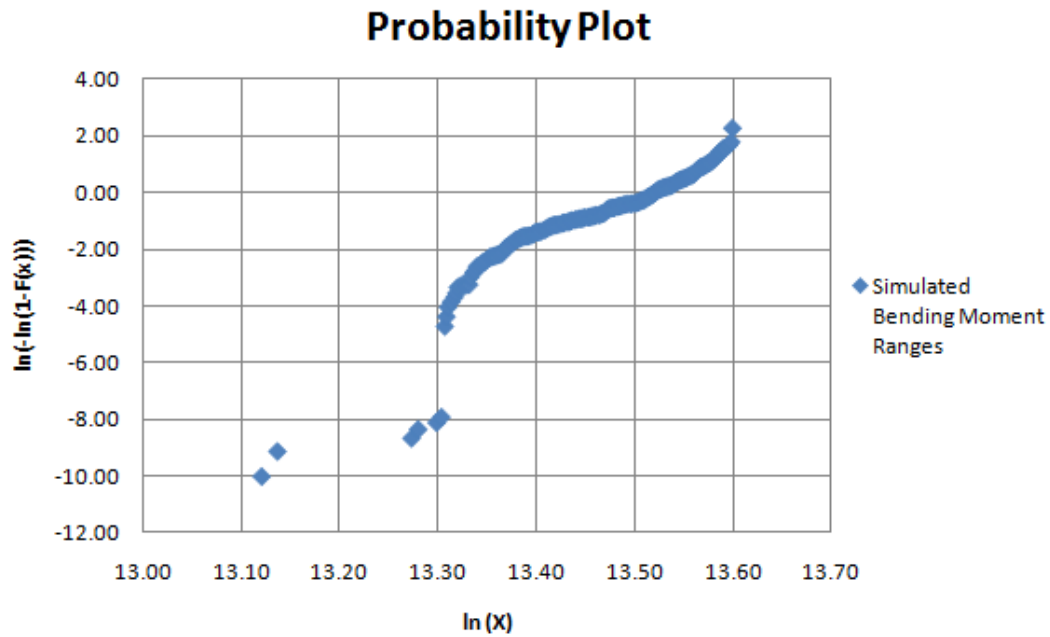


Figure 4.11 – Cumulative distribution of simulated BMRs

This bin is defined by $E[U_8] = 1.50 - 1.60$ m/s and $I_T = 0.05 - 0.10$, meaning all of the 8-hour records that were placed in this bin had an 8-hour mean current velocity $E[U_8]$ between 1.50 and 1.60 m/s and a turbulence intensity I_T between 0.05 and 0.10. The cumulative number of occurrences is obtained by adding the number of occurrences at the given BMR and lower BMR values.

It is of interest to understand why there are only a few outliers at the lower tail. These smaller BMRs can be attributed to the bending moment time histories transitioning from one 30 minute period to another. For example, an examination of Figure 4.10 shows that there is a relatively small BMR in the transition from the last maximum bending moment in the first 30 minute interval to the first minimum bending moment in the second 30 minute interval.

4.2.4.2 Cumulative distribution function

A 2-parameter Weibull model is used to model the cumulative probability of the BMRs in each bin. The probability density function for the Weibull distribution is given by

$$f(x) = ba^{-b}x^{(b-1)}\exp\left(-\left(\frac{x}{a}\right)^b\right) \quad (3.3-3)$$

where the constants a and b are the scale and shape factors, respectively. These constants are determined so as to fit the BMRs contained within each bin using Matlab's curve fitting program. After the determination of the constants a and b , the cumulative distribution function (CDF), which is the integral of the probability density function (Equation 3.3-3) is given by Equation 3.3-4.

$$F(x) = 1 - \exp \left(- \left(\frac{x}{a} \right)^b \right) \quad (3.3-4)$$

The CDF is plotted and shown in Figure 4.12 along with the actual cumulative distribution of the simulated BMRs.

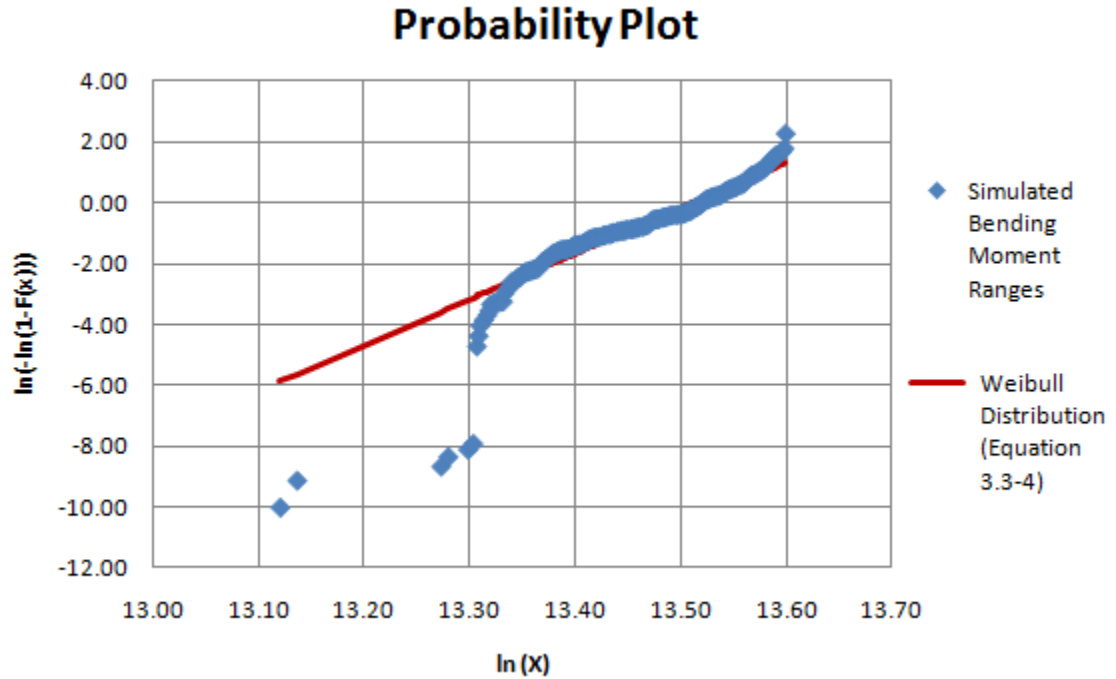


Figure 4.12 - Cumulative Distribution Function

The Weibull model fit appears to be very satisfactory at the upper tail of the distribution where the BMRs cause the most damage to the rotor blades. It can be seen from Table 4.12 that the outliers at the lower tail represent one occurrence each and hence, they do not contribute to fatigue damage to any extent.

4.2.4.3 Probability Content

With the number of 8-hour records known in each bin, the BMR (x-axis) is

divided into equal intervals based on the number of 8-hour records (Figure 4.13). The probability content for each interval is then calculated using the CDF (Equation 3.3-4). The probability content is defined as the probability of a given BMR occurring in a given interval. The probability content is then used to determine the number of cycles in any given interval of BMRs.

For example, in a typical bin it is found that there are six 8-hour records, and the largest and smallest BMRs are respectively 997,000 N-m and 499,000 N-m. The coefficients a and b for this bin are determined to be 737,879 and 14.9799 using the probability density function given by Equation 3.3-3. The difference between these BMRs is 498,000 N-m. The difference is then divided by six, which represents the number of 8-hour records in this bin, giving a BMR interval of 83,000 N-m. The first interval is defined by limits 1 and 2, and the second interval by limits 2 and 3, and so on (Table 4.2 and Figure 4.13). The BMR for each limit is substituted into the CDF (Equation 3.3-4) to obtain the cumulative probability $F(x)$ and the results are shown in Table 4.2.

Table 4.2 – Cumulative probabilities for BMR interval limits for one bin

Limit #	BMR, X (N-m)	$\ln(X)$	Cumulative Probability, $F(x)$ (Equation 3.3-4)	$\ln(-\ln(1-F(x)))$
1	499,000	13.1204	0.0028	-5.86
2	582,000	13.2742	0.0282	-3.55
3	665,000	13.4075	0.1899	-1.56
4	748,000	13.5252	0.7066	0.20
5	831,000	13.6304	0.9973	1.78
6	914,000	13.7256	1.0000	3.21
7	997,000	13.8125	1.0000	4.50

The discretization can be seen in the Figure 4.13 below.

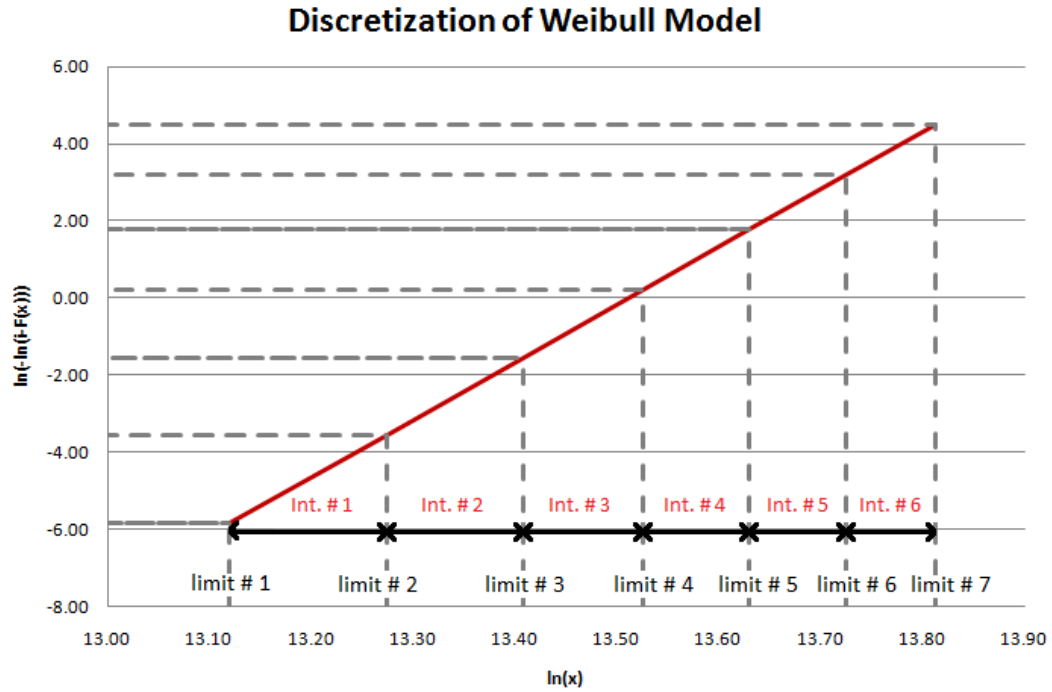


Figure 4.13 – Discretization of the cumulative distribution function for BMRs in a typical bin

Next, the average value of the BMR limits is determined for each interval (Table 4.3). Then, the probability content for each average value representing the interval is determined by taking the difference of the cumulative probabilities associated with the lower and upper limits shown in Table 4.2. The total number of cycles in this particular bin has already been determined from the rainflow counting method to be 15,375. The probability content (Table 4.3) is now multiplied by the total number of cycles to obtain the number of cycles corresponding to a given BMR interval. It is important to note that the number of cycles in a given interval is only for a one month period (not the design life of 20 years), therefore the values of these number are not rounded to the nearest whole cycle to prevent a large rounding error.

Table 4.3 – Number of cycles for Bin #6 containing 15,375 cycles

Interval #	Average Value of BMR X (N-m)	Probability Content	Number of Cycles
1	540,500	0.0253	389.49
2	623,500	0.1617	2,486.45
3	706,500	0.5167	7,945.02
4	789,500	0.2907	4,469.47
5	872,500	0.0027	40.79
6	955,500	0.0000	0.00

This procedure is repeated for each bin, resulting in a total of 11 tables similar to Table 4.3, each containing a set of BMRs along with the corresponding number of cycles.

The BMRs with their corresponding number of cycles from all 11 bins considered in the study are combined and arranged in descending order according to the magnitude of the BMRs. This can be seen in the first and third rows of Table 4.4. The fourth column in Table 4.4 is obtained by dividing the BMR by the section modulus. The number of exceeding cycles for a given BMR is then determined by summation of the number of cycles at or above the given BMR as shown in the Table 4.4. The number of exceeding cycles in the design life is calculated as the number of exceeding cycles times the design life, which is 20 years which equals 240 months. The design life in years is converted to months because the number of exceeding cycles is for a one month period.

Table 4.4 – Number of Exceeding Cycles in Design Life (Appendix C)

X (N-m)	X (kN-m)	Number of Cycles	Number of Exceeding Cycles	Number of Exceeding Cycles in Design Life
1,037,150	1037	8.27	8.268E+00	1.984E+03
1,021,000	1021	0.00	8.268E+00	1.984E+03
1,004,075	1004	0.00	8.268E+00	1.984E+03
.
.
.
581,000	581	1043.22	1.581E+05	3.793E+07
540,500	541	389.49	1.584E+05	3.803E+07
524,525	525	339.56	1.588E+05	3.811E+07
493,000	493	121.36	1.589E+05	3.814E+07

The BMRs and number of exceeding cycles are plotted as shown in Figure 4.14 below.

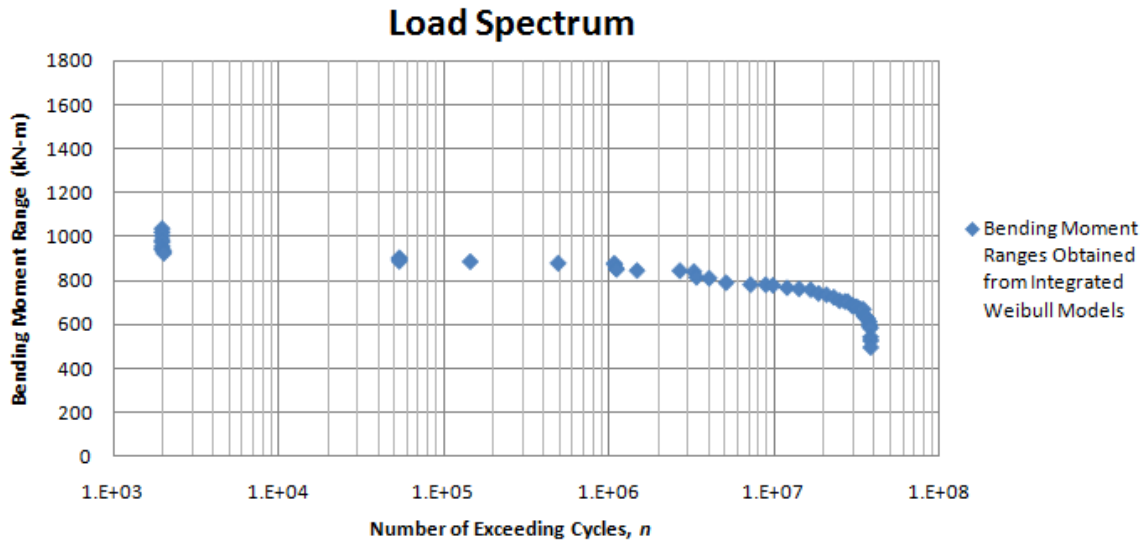


Figure 4.14 – Integration of BMR distributions over the design life

4.2.5 Characteristic bending moment range distribution

An idealized characteristic BMR distribution is assumed to best represent the simulated BMR distribution

$$X = X_a + k_R X_c \left(1 - \frac{\log(n)}{\log(3N_r)} \right) \quad (3.3-5)$$

where n represents the number of exceeding cycles, N_r is the number of rotor blade fatigue cycles in the design life T_L , X_a is the adjustment BMR value, k_R is a scaling factor, and X_c is the characteristic bending moment. The number of rotor blade fatigue cycles N_r is calculated knowing the number of revolutions of the rotor blade per minute f_r and given by $N_r = T_L * f_r = 7.36 * 10^7$ cycles. There were no bending moments ranges less than 485,750 N-m so the characteristic BMR distribution is adjusted (shifted up) by an amount $X_a = 485,750$ N-m. The scaling factor k_R is calibrated so that the characteristic BMR distribution (Equation 3.3-5) yields the same fatigue damage as the damage predicted by the integrated Weibull modeling (Figure 4.14) of the simulated bending moment time histories (Figure 4.10). The scaling factor k_R is determined to be 1.409 and the procedure of calibrating k_R is illustrated in section 4.6.2. The characteristic bending moment X_c is defined by the Danish code (Dansk Ingeniørforening, 1992) and is given by

$$X_c = \frac{\rho_w}{2} w^2 c C_L \frac{R^2}{3} \quad (3.3-6)$$

where ρ_w represents the density of water (1000 kg/m³), R is the radius of the rotor blade, C_L is the lift coefficient, c is the characteristic chord length, and w is the reference wave-current velocity. The radius of the rotor blade R is taken as the distance from the center of the hub to the tip of the blade and is equal to 10 meters. The lift coefficient C_L and characteristic chord length c , both taken at a distance of $2R/3$ from the center of the hub are 1.28 and 1.685 meters, respectively. The reference wave-current velocity w is assumed to be given by

$$w^2 = \left(\frac{4\pi}{3} f_r R \right)^2 + v_o^2 \quad (3.3-7)$$

where v_o is the velocity at stalling which is taken at 1.50 m/s.

4.3 FATIGUE STRENGTH AND ε -N CURVE

4.3.1 Resistance and stiffness of composite laminates

A regression analysis of published data (pairs of ε - N) is performed using a linear model. A total of 81 pairs of strain and number of cycles to failure (ε , N) from laboratory tests on a composite material are used in the analysis (Echtermeyer et al. 1993, 1994). The data are digitized from the plot given by Ronold et al. (1999). Out of the 81 pairs, 78 pairs are obtained using a digitizer and the results are shown below in Table 4.5.

Table 4.5 – 78 Pairs of $\log \epsilon$ and $\log N$

Pair #	$\log N$	$\log \epsilon$	Pair #	$\log N$	$\log \epsilon$	Pair #	$\log N$	$\log \epsilon$
1	1.29	-1.74	27	3.08	-2.02	53	4.92	-2.20
2	1.32	-1.77	28	3.33	-1.93	54	4.93	-2.23
3	1.61	-1.85	29	3.43	-2.12	55	4.93	-2.20
4	1.74	-1.77	30	3.44	-2.00	56	4.94	-2.22
5	1.79	-1.79	31	3.67	-2.12	57	5.06	-2.16
6	1.80	-1.78	32	3.77	-2.06	58	5.24	-2.26
7	1.81	-1.84	33	3.83	-2.12	59	5.25	-2.27
8	1.89	-1.92	34	3.85	-2.01	60	5.25	-2.26
9	1.93	-1.78	35	3.91	-2.12	61	5.25	-2.19
10	2.00	-1.81	36	3.95	-2.02	62	5.37	-2.23
11	2.01	-1.90	37	3.99	-2.10	63	5.38	-2.25
12	2.04	-1.93	38	4.03	-2.12	64	5.49	-2.23
13	2.05	-1.84	39	4.07	-2.02	65	5.55	-2.27
14	2.20	-1.81	40	4.09	-2.12	66	5.66	-2.27
15	2.20	-1.80	41	4.13	-2.02	67	5.72	-2.30
16	2.24	-1.83	42	4.15	-2.12	68	5.72	-2.25
17	2.32	-1.85	43	4.23	-2.10	69	5.79	-2.24
18	2.32	-1.83	44	4.23	-2.06	70	5.90	-2.25
19	2.36	-1.77	45	4.35	-2.07	71	5.94	-2.27
20	2.40	-1.86	46	4.51	-2.12	72	5.95	-2.29
21	2.41	-1.83	47	4.52	-2.12	73	6.00	-2.35
22	2.48	-1.98	48	4.59	-2.18	74	6.06	-2.25
23	2.83	-1.88	49	4.59	-2.12	75	6.12	-2.29
24	2.89	-1.83	50	4.60	-2.20	76	6.18	-2.31
25	3.03	-1.91	51	4.65	-2.11	77	6.21	-2.27
26	3.07	-1.88	52	4.87	-2.20	78	6.60	-2.35

The composite is a polyester laminate reinforced by five layers of combined woven glass roving and chopped strand mat with fibers oriented at 0/90 during testing and with some fibers in the load direction (Echtermeyer et al. 1993, 1994). The observed pairs of ϵ - N are plotted as shown below in Figure 4.15.

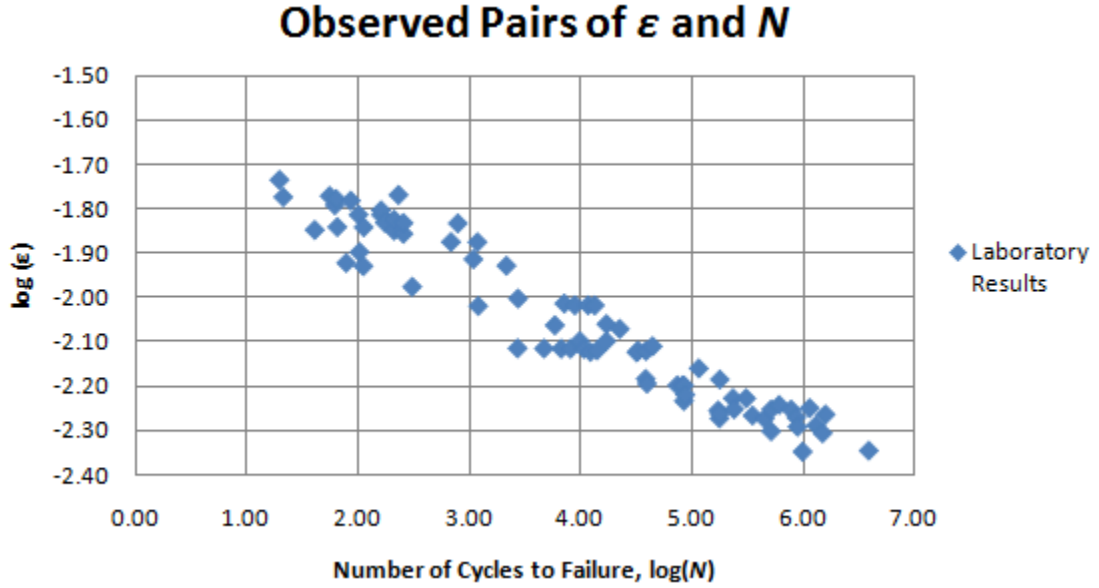


Figure 4.15 – Strain amplitude versus number of cycles to failure

The strain is reported as the strain amplitude, which is half of the strain range. The ϵ - N curve that gives the number of cycles N to failure for the rotor blade is given by

$$\log N = E[\log K] - E[m]\log \epsilon + E[e] \quad (3.4-1)$$

where $\log K$ and m are material constants, e represents the horizontal residuals, and $E[]$ represents the expected value (Ronold et al., 1999). It should be noted that this ϵ - N relationship (Equation 3.4-1) ignores the effect of non-zero mean stresses. The effect of mean stress will be considered in Section 4.5. During the test, the strain was kept constant in the determination of the number of cycles to failure N . Therefore, the uncertainty lies in $\log N$ (Echtermeyer et al., 1993) and the horizontal residuals represent the uncertainty in the testing. The horizontal residuals are simply the distances from each ϵ - N pair to the fitted ϵ - N curve (Equation 3.4-1) and represent local variations from the various test

specimens. A linear regression is performed to obtain the coefficients $E[\log K]$ and $E[m]$ and the results are given as:

$$E[\log K] = -12.2978$$

$$E[m] = 7.8794$$

$$E[e] = -0.004$$

These values are substituted into Equation 3.4-1 in order to obtain the best-fit ϵ - N curve and shown below in Figure 4.16.

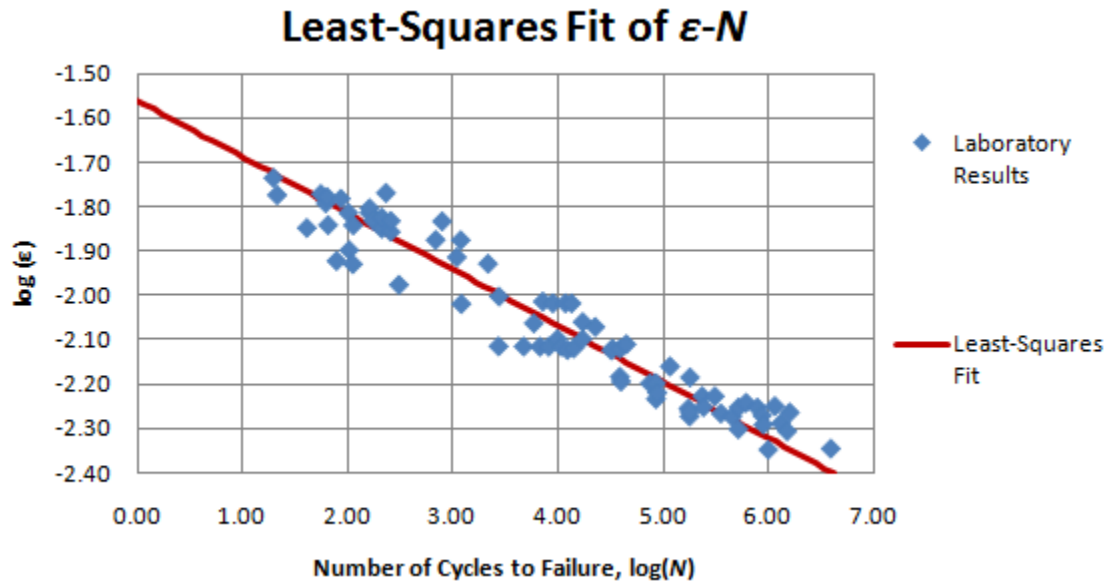


Figure 4.16 – Least Squares Fit of ϵ - N Data (Appendix C)

The standard deviation of the residuals is calculated as

$$D[e] = \sqrt{\frac{1}{M-1} \sum_{i=1}^M (e_i - E[e])^2} \quad (3.4-3)$$

where $D[]$ represents the standard deviation and M represents the total number of ϵ - N pairs. The standard deviation of the residuals is found to be $D[e] = 0.398$.

4.3.2 Standard deviations of $\log K$ and m using the jackknife technique

The jackknife technique is used here to obtain values for the standard deviation of $\log K$ and m . These values are used later in the reliability analysis. The jackknife technique involves removing one pair of ε and N at a time and recalculating the coefficients $\log K$ and m (Equation 3.4-1). For example, the first pair of ε and N is removed and the coefficients $\log K$ and m are calculated by performing another linear regression using Equation 3.4-1. The first pair of ε and N is then placed back into the data set and the second pair of ε and N is removed. The coefficients $\log K$ and m are calculated again, and this process is repeated until every pair of ε and N has been removed and replaced in the data set. This results in several values for $\log K$ and m . The standard deviations are then calculated by using Equations 3.4-4 and 3.4-5 below.

$$D[\log K] = \sqrt{\frac{M-1}{M} \sum_{i=1}^M ((\log(K))_i - E[\log(K)])^2} \quad (3.4-4)$$

$$D[m] = \sqrt{\frac{M-1}{M} \sum_{i=1}^M (m_i - E[m])^2} \quad (3.4-5)$$

The standard deviations for $\log K$ and m obtained using the jackknife technique are shown below.

$$D[\log K] = 0.4810$$

$$D[m] = 0.2286$$

4.3.3 Correlation coefficient

Given that $\log K$ and m are fitting parameters for the ε - N curve, the coefficient of correlation between the two variables is given by

$$\rho = \frac{\frac{M-1}{M} \sum_{i=1}^M [(\log(K))_i - E[\log(K)]] * [m_i - E[m]]}{D[\log K] * D[m]} \quad (3.4-6)$$

The correlation coefficient ρ between $\log K$ and m is calculated to be -0.9956

4.4 FATIGUE DAMAGE FOR MCT ROTOR BLADES

4.4.1 Miner's rule for cumulative damage

Two fatigue damage predictions are made for every bin based on Miner's rule, one based on the simulated BMRs (actual damage) and another based on the Weibull model (Table 4.3). Miner's rule for the fatigue damage is defined as

$$D = \sum_{i=1} \frac{\Delta n(S_i)}{N(S_i)} \quad (3.5-1)$$

where Δn represents the number of stress cycles occurring at a given stress range S_i . In order to obtain the stress range, the BMR is divided by the section modulus W ($S = X/W$) of the rotor blade. For the purposes of comparing the actual damage and damage predicted by the Weibull model, an initial section modulus W of 0.007 m^3 is selected for the rotor blade, which will be calibrated in Section 5.4 in order to obtain the desired reliability.

The ε - N curve is used to obtain the number of cycles to failure, $N(S_i)$ for a given stress range S_i . The strain amplitude ε is easily converted to the equivalent stress range from the relationship $S = 2E\varepsilon$. Equation 3.4-1 is rewritten in terms of stress to calculate $N(S_i)$. The residual term e is left out of the equation because it is essentially zero.

$$\log N(S_i) = E[\log K] - E[m] \log \left(\frac{S_i}{2E} \right) \quad (4.4.1-1)$$

4.4.2 Damage calculations based on simulated bending moment ranges

The computations for the total damage is illustrated for one of the bins (Bin #6) and shown in Table 4.6 below. There are 15,375 BMRs contained in this bin. For brevity, only selected values of the BMRs are shown in Table 4.6.

Table 4.6 - Bin # 6: Damage Calculations Using Simulated (Actual) BMRs (Appendix C)

X (N-m)	Stress Range (Pa)	Number of Cycles	Number of Cycles to Failure, $N(S_i)$ (Equation 4.4.1-1)	Damage, D (Equation 3.5-1)
499,000	71,285,714	1	5.20E+10	1.92E-11
507,000	72,428,571	1	4.59E+10	2.18E-11
581,000	83,000,000	1	1.57E+10	6.37E-11
.
.
.
982,000	140,285,714	1	2.51E+08	3.98E-09
997,000	142,428,571	1	2.23E+08	4.49E-09
			Total Damage	5.72E-06

Each BMR is first divided by the section modulus W to obtain the stress range. The values for $\log K$ and m are known from the least-squares regression of the laboratory ε - N data (Figure 4.16). The number of cycles to failure is calculated using Equation 4.4.1-1 for any given stress range S_i . The resulting damage due to the stress range S_i is then calculated using Miner's rule (Equation 3.5-1). The cumulative damage is then given by the summation of all of the damages due to the individual stress ranges.

4.4.3 Damage calculations based on the two-parameter Weibull model

An example of the damage predicted by the Weibull model is shown in Table 4.7 below which is an extension of Table 4.3. Equation 4.4.1-1 is again used to calculate the

number of cycles to failure and the damage by using Miner's rule (Equation 3.5-1).

Table 4.7 – Bin # 6: Damage Calculations Using Weibull Model (Appendix C)

Interval	Average Value of BMR (N-m)	Stress Range (Pa)	Probability Content	Number of Cycles, Δn	Number of Cycles to Failure, $N(S_i)$ (Equation 4.4.1-1)	Damage, D (Equation 3.5-1)
1	540,500	77,214,286	0.025	389	2.77E+10	1.40E-08
2	623,500	89,071,429	0.162	2486	9.00E+09	2.76E-07
3	706,500	100,928,571	0.517	7945	3.36E+09	2.36E-06
4	789,500	112,785,714	0.291	4469	1.40E+09	3.19E-06
5	872,500	124,642,857	0.003	41	6.37E+08	6.40E-08
6	955,500	136,500,000	0.000	0	3.11E+08	9.34E-16
				Total Damage		5.91E-06

4.4.4 Comparison of fatigue damage predictions

A comparison of the damage predicted from the simulated BMRs (actual damage) and the damage predicted by the Weibull model is shown in the histogram in Figure 4.17.

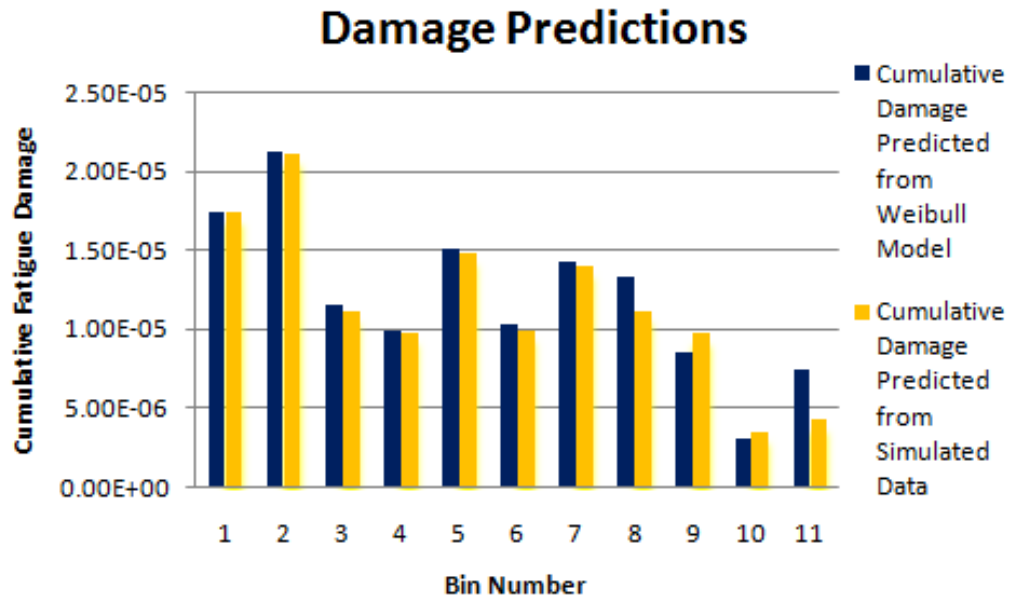


Figure 4.17 – Comparison of predicted cumulative damage

The primary reason that the damages predicted vary from bin to bin can be attributed to the number of 8-hour records contained within each bin. For example, there are ten 8-hour records in bin number one and only two 8-hour records in bin number ten, hence, there is much more damage predicted from bin number one.

The ratio between the two fatigue damage calculations F_M is calculated for each bin and defined as the random factor.

$$F_M = \frac{\text{cumulative damage predicted by simulated BMRs}}{\text{cumulative damage predicted by Weibull model}} \quad (3.5-4)$$

The mean and standard deviation of the random factor F_M considering all bins is calculated for the purposes of the reliability analysis (Chapter 5) and the results are shown below.

$$E[F_M] = 0.959 \quad D[F_M] = 0.155$$

The results show that the Weibull model tends to over predict the damage by a factor of $1/0.959 = 1.043$. The mean and standard deviation of the random factor are used in the reliability analysis (Chapter 5) to adjust for the over prediction of the Weibull model.

4.5 EFFECT OF NON-ZERO MEAN STRESS ON FATIGUE DAMAGE

The effect of non-zero mean stress is taken into consideration in the present study. The stress ranges do not have a zero mean, therefore, the Morrow equation (Equation 4.5-1) is utilized in order to calculate the equivalent stress range that has a zero mean (Dowling, 2007). The equivalent stress range S_{eq} is given by

$$S_{eq} = \frac{S_i}{1 - \frac{S_m}{S_o}} \quad (4.5-1)$$

where S_i is any given stress range, S_m is the mean stress range and S_o is the static strength. The static strength S_o for the polyester laminate is assumed to be 322 MPa according to Echtermeyer et al. (1993). The mean stress range S_m is calculated as the mean value of the BMRs $E[X_m]$ as illustrated in Section 4.2.2 divided by the section modulus W . The section modulus is initially assumed to be 0.007 m^3 (this section modulus is calibrated in Chapter 5), which yields a value of $S_m = 17.0 \text{ MPa}$.

The value of S_{eq} will be used in place of S_i in Equation 4.4.1-1 to predict the fatigue damage, giving Equation 4.5-2.

$$\log N(S_{eq}) = E[\log K] - E[m] \log \left(\frac{S_{eq}}{2E} \right) \quad (4.5-2)$$

Using the equivalent stress range (larger stress range) will result in a lower number of cycles to failure and hence, more damage.

The fatigue damage over the 20 year design life without considering the effect of non-zero mean stress is calculated to be 0.0189 whereas the fatigue damage considering the effect of non-zero mean stress is computed to be 0.0290. This shows the importance of considering the effect of mean stress as there was $0.0290/0.0189 = 1.54$ times, or 54% more damage when the effect of non-zero mean stress is taken into consideration. This factor is specifically for a section modulus of 0.007 m^3 . To put things into perspective, if the section modulus were decreased to 0.006 m^3 or increased to 0.008 m^3 then the factors would be 1.65 and 1.45, respectively.

4.6 MODEL UNCERTAINTY

4.6.1 Limit state function

Reliability against fatigue failure of the MCT rotor blade in flapwise bending is analyzed in the present study for the cyclic loading caused by marine current. For this purpose, a limit state function is defined as

$$g(x) = 1 - F_M D(\mathbf{X}) \quad (4.6.1-1)$$

where $D(\mathbf{X})$ represents the cumulative damage predicted based on the integrated effects of the Weibull models from all of the bins as presented in Table 4.8. \mathbf{X} is a vector that contains the stochastic variables ($\log K$, m , e , F_M , and X_m) which have uncertainty in the modeling. F_M represents the bias and uncertainty in the cumulative damage prediction from the Weibull models. Failure is defined to occur when the limit state function $g(x) \leq 0$.

4.6.2 Calibration of the scaling factor, k_R

Up to this point, the damage has been calculated based on the simulated BMRs and the 11 two-parameter Weibull models (Figure 4.14). Now, the 11 two-parameter Weibull models that have been integrated are fitted by using the characteristic BMR distribution (Equation 3.3-5) so that the damage may be calculated. In order to obtain the damage due to the characteristic BMR distribution, k_R must first be calibrated. The scaling factor is calibrated so as to have the characteristic BMR and the corresponding damage to be the same as that predicted by the integration of the 11 Weibull models.

All of the bins are integrated as illustrated in Section 4.2.4.3 to obtain an ordered history of the stress ranges over the design life of 20 years (Table 4.4 and Figure 4.14). Table 4.8 is an extension of Table 4.4 and illustrates the calculation of the damage predicted by the integration of the Weibull models from all of the 11 bins. Miner's rule for cumulative damage (Equation 3.5-1) is used in conjunction with the ε - N curve (Equation 4.5-2) to obtain the cumulative fatigue damage.

Table 4.8 - Compound BMR Damage Calculations (Appendix C)

BMR, X (N-m)	SR, S (Pa)	Equivalent SR, S_{eq} (Pa) (Equation 4.5-1)	Number of Cycles in Design Life, Δn	Number of Cycles to Failure, N (Equation 4.5-2)	Damage, D (Equation 3.5-1)
1.037E+06	1.482E+08	1.564E+08	1.984E+00	1.063E+08	1.867E-05
1.021E+06	1.459E+08	1.540E+08	0.000E+00	1.203E+08	0.000E+00
1.004E+06	1.434E+08	1.515E+08	1.144E+00	1.372E+08	8.336E-09
.
.
.
5.245E+05	7.439E+07	7.912E+07	8.150E+04	2.288E+10	3.563E-06
4.930E+05	7.043E+07	7.437E+07	2.913E+04	3.728E+10	7.813E-07
4.858E+05	7.939E+07	7.327E+07	9.480E+04	4.190E+10	2.263E-06
Cumulative Fatigue Damage					0.02798

A similar table (Table 4.9) is created based on the characteristic BMR distribution (Equation 3.3-5).

Table 4.9 – Characteristic BMR Distribution Damage Calculations (Appendix C)

Number of Exceeding Cycles, n	Number of Cycles in Interval, Δn	BMR, X (N-m) (Equation 3.3-5)	Average SR, S (Pa)	Equivalent SR, S_{eq} (Pa) (Equation 4.5-1)	Number of Cycles to Failure, N (Equation 4.5-2)	Damage, D (Equation 3.5-1)
1.00E+01	1.00E+01	1.651E+06	2.324E+08	2.454E+08	3.058E+06	3.271E-06
2.00E+01	1.00E+01	1.603E+06	2.270E+08	2.397E+08	3.681E+06	2.717E-06
3.00E+01	1.00E+01	1.575E+06	2.236E+08	2.361E+08	4.147E+06	2.411E-06
.
.
.
2.18E+08	1.00E+06	4.867E+05	6.950E+07	7.339E+07	4.139E+10	2.416E-05
2.19E+08	1.00E+06	4.863E+05	6.946E+07	7.334E+07	4.160E+10	2.404E-05
2.20E+08	1.00E+06	4.860E+05	6.941E+07	7.329E+07	4.181E+10	2.392E-05
2.21E+08		4.857E+05	Cumulative Fatigue Damage			0.02798

Miner's rule (Equation 3.5-1) is again used in conjunction with the ε - N curve (Equation 4.5-2) to calculate the cumulative fatigue damage. The value of k_R is iterated until the cumulative fatigue damage predicted by the characteristic BMR equals the damage predicted by the integration of all the Weibull models as shown in Tables 4.8 and 4.9. The scaling factor k_R is calibrated to be 1.409. This is substituted into the characteristic BMR distribution (Equation 3.3-5) and plotted in Figure 4.18.

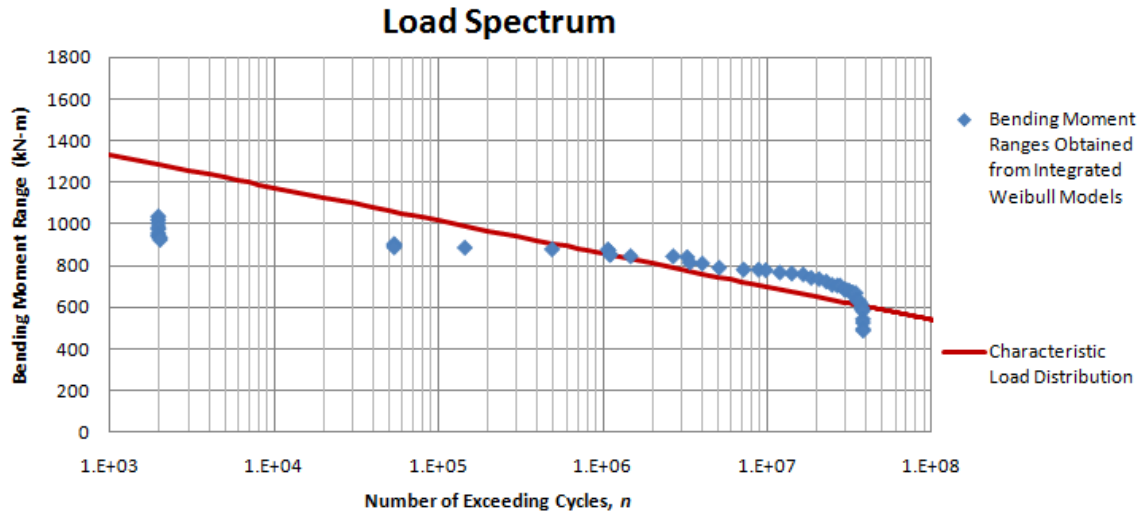


Figure 4.18 – Characteristic BMR distribution

For any given BMR interval, the number of cycles in a given interval can be calculated by taking the difference of the number of exceeding cycles at upper and lower limits the given interval. The characteristic BMR distribution may be utilized for any BMR greater than $X_a = 485,750$ N-m.

This characteristic BMR distribution is used in the calibration of partial safety factors (Chapter 6).

CHAPTER 5

RELIABILITY ANALYSIS APPLIED TO MCT ROTOR BLADE FATIGUE DAMAGE

5.1 INTRODUCTION

The first-order reliability method is utilized in the present study to calibrate the section modulus of the MCT rotor blade that is associated with an acceptable probability of failure for the 20 year design life. The method involves calculating the most likely values of all basic stochastic variables ($\log K$, m , etc,...) at failure used in the modeling of the cumulative fatigue damage. These values are then used to calculate the reliability index, which gives the probability of failure.

The mean and standard deviation of several basic stochastic variables have been calculated in Chapter 4 and used to predict the cumulative fatigue damage in the MCT rotor blade based on Miner's rule. The mean values for the stochastic variables do not necessarily represent the true values. The cumulative probability of any value of a given variable may be found by calculating the Z-values (Equation 3.6-2) under the assumption that the variables are normally distributed. The reliability index can then be calculated for a set of basic stochastic variables and is used to calculate the probability of failure. The section modulus W is still considered to equal 0.007 m^3 for now, but is calibrated in Section 5.4 in order to obtain a desired reliability index.

5.2 DESIGN POINT AND Z-VALUE

The design point \mathbf{X}^* is a vector containing the design points of the five basic stochastic variables described in Chapter 4 and represents the most likely values of the basic stochastic variables at failure.

$$\mathbf{X}^* = \begin{bmatrix} \log K^* \\ m^* \\ e^* \\ X_m^* \\ F_M^* \end{bmatrix} \quad (5.2-1)$$

The design point of each variable will be calculated during the first-order reliability method as described later in Section 5.4. With the mean and standard deviation of each variable known, the cumulative probability of each design point occurring may be found by transforming the distribution of the variables into a standard normal distribution. The standard normal distribution is a normal distribution where the mean equals zero and the standard deviation equals one. The distributions are transformed so that the standard normal cumulative distribution table may be used in order to find the probability of failure. The Z-value (found in the standard normal cumulative distribution table) of a given variable is defined as

$$Z = \frac{\mathbf{X}^* - E[\mathbf{X}]}{D[\mathbf{X}]} \quad (3.6-2)$$

where $E[\mathbf{X}]$ and $D[\mathbf{X}]$ are the mean and standard deviation vectors of the variables (Ayyub et al., 1997). The probability of failure is then found as

$$P_F = 1 - \Phi(Z) \quad (5.2-2)$$

where Φ is the notation for the standard normal cumulative distribution function. The values of $\Phi(Z)$ can be found in the standard normal cumulative distribution table (Table

A-1, Ayyub et al., 1997).

5.3 LIMIT STATE FUNCTION

The limit state function $g(x)$ is defined as one minus the random factor times the cumulative fatigue damage calculated from the Weibull model $D(\mathbf{X}^*)$ as shown in Equation 3.6-1.

$$g(x) = 1 - F_M^* D(\mathbf{X}^*) \quad (3.6-1)$$

This equation is the same as Equation 4.6.1-1 but using the design points rather than the mean values. Failure occurs when the limit state function becomes less than or equal to zero. To recap from Chapter 4, the ε - N curve (including the residual term) is given by

$$\log N(S_{eq}) = E[\log K] - E[m] \log \left(\frac{S_{eq}}{2E} \right) + E[e] \quad (4.5-2)$$

The design point ε - N curve is obtained by replacing the basic stochastic variables with the design point variables. The design point ε - N curve becomes

$$\log N^*(S_{eq}) = \log K^* - m^* \log \left(\frac{S_{eq}}{2E} \right) + e^* \quad (5.3-1)$$

where $\log K^*$, m^* , and e^* are design point values and represent the most likely values of the stochastic variables at failure. The mean and standard deviation of each basic stochastic variable has already been calculated in Chapter 4 and is reproduced in Table 5.1. A column for the design point, which is denoted by using an asterisk, for each variable is also created. Initially, the design points are set equal to the mean values of each variable, but will be calculated later.

Table 5.1 – Summary of Mean and Standard Deviations of Stochastic Variables from Chapter 4

X	$E[X]$	$D[X]$	X^*
$\log K$	-12.2978	0.4810	-12.2978
m	7.8794	0.229	7.8794
e	-0.004	0.398	-0.004
F_M	0.959	0.155	0.959
X_m	119339	82573	119339

The Z-value (found on the standard normal distribution table) is calculated for each variable from Equation 3.6-2. The Z-value of each variable can be used to calculate the cumulative probability of the design point.

A correlation matrix $[R]$ is also assembled to account for any correlations that exist between all five stochastic variables. Out of the five stochastic variables, the only correlation is between $\log K$ and m , due to the fact that these are fitting parameters for the same curve (Equation 3.4-1). The correlation coefficient of -0.9956 was calculated as described in Section 4.3.3. The correlation matrix R is given by

$$\begin{array}{c}
 \log K \\
 m \\
 e \\
 F_M \\
 X_m
 \end{array}
 \begin{bmatrix}
 \log K & m & e & F_M & X_m \\
 1 & -0.9956 & 0 & 0 & 0 \\
 -0.9956 & 1 & 0 & 0 & 0 \\
 0 & 0 & 1 & 0 & 0 \\
 0 & 0 & 0 & 1 & 0 \\
 0 & 0 & 0 & 0 & 1
 \end{bmatrix}$$

Table 5.2 is created using Microsoft Excel which is an extension of Table 5.1 that consists of the mean, standard deviation, design point (initially set equal to the mean values), and Z-value of each basic stochastic variable, along with the correlation matrix.

Table 5.2 - Basic Stochastic Variables

X	$E[X]$	$D[X]$	X^*	Z	Correlation Matrix, $[R]$				
$\log K$	-12.2978	0.4810	-12.2978	0	1	-0.9956	0	0	0
m	7.8794	0.229	7.8794	0	-0.9956	1	0	0	0
e	-0.004	0.398	-0.004	0	0	0	1	0	0
F_M	0.959	0.155	0.959	0	0	0	0	1	0
X_m	119339	82573	119339	0	0	0	0	0	1

Naturally, if the design point is equal to the mean value, the Z -value equals zero (Equation 3.6-2). The damage is calculated as described in Table 4.8, but using the design point ε - N curve (Equation 5.3-1) rather than the ε - N curve (Equation 4.5-2) described in Chapter 4. Table 5.3 (Appendix D) illustrates a few of the calculations.

Table 5.3 – Compound BMR Damage Calculations Using the Design Point ε - N Curve

BMR, X (N-m)	SR, S (Pa)	Equivalent SR, S_{eq} (Pa) (Equation 4.5-1)	Number of Cycles in Design Life, Δn	Number of Cycles to Failure, N^* (Equation 5.3-1)	Damage, D (Equation 3.5-1)
1.037E+06	1.482E+08	1.564E+08	1.984E+03	1.054E+08	1.883E-05
1.021E+06	1.459E+08	1.540E+08	0.000E+00	1.193E+08	0.000E+00
1.004E+06	1.434E+08	1.515E+08	1.144E+00	1.361E+08	8.405E-09
.
.
.
5.405E+05	7.721E+07	8.153E+07	9.348E+04	1.791E+10	5.219E-06
5.245E+05	7.493E+07	7.912E+07	8.150E+04	2.269E+10	3.592E-06
4.930E+05	7.043E+07	7.437E+07	2.913E+04	3.697E+10	7.878E-07
Cumulative Fatigue Damage					0.0282

The minor difference in the total fatigue damages calculated in Tables 4.8/4.9 and 5.3 can be attributed to the fact that Tables 4.8/4.9 ignored the effect of the residual term e .

The cumulative fatigue damage from Table 5.3 and the design point random factor F_M^* from Table 5.2 are substituted into the limit state function (Equation 3.6-1) which yields a value of 0.9729. Failure does not occur until the limit state function is less than or equal to zero, therefore, the MCT rotor blade is far from failure due to fatigue.

The solver function in Microsoft Excel may be used to solve for the design point values \mathbf{X}^* that will yield a value for the limit state function $g(x)$ to be zero. There are an infinite number of solutions that will satisfy this requirement; therefore, the reliability index needs to be included in the analysis which is discussed in Section 5.4.

5.4 RELIABILITY INDEX

The reliability is the complement of the probability of failure P_F and is defined as

$$P_F = P[g(x) \leq 0] \quad (5.4-1)$$

where $P []$ represents the probability. The probability of failure P_F can be expressed in terms of the reliability index β .

$$\beta = -\Phi^{-1}(P_F) \quad (5.4-2)$$

The reliability index can be thought of as the combination of all of the Z-values as calculated in Equation 3.6-2 and tabulated in Table 5.2. The reliability index is essentially the square root of the sum of the squares of the z-values. The precise definition for the reliability index includes correlations between the variables and is given by Equation 5.4-3 (Low et al., 2002)

$$\beta = \min \sqrt{\left[\frac{x_i - m_i}{\sigma_i} \right]^T [\underline{R}]^{-1} \left[\frac{x_i - m_i}{\sigma_i} \right]} \quad (5.4-3)$$

where x_i represents the design point of the stochastic variables ($\log K$, m , e , F_M , and X_m), m_i and σ_i are the mean and standard deviations of the stochastic variables, and $[R]$ is the correlation matrix. Rewriting the Equation 5.4-3 using the notation used in the present study yields Equation 3.6-3.

$$\beta = \min \sqrt{\left[\frac{\mathbf{X}^* - E[\mathbf{X}]}{D[\mathbf{X}]} \right]^T [\underline{R}]^{-1} \left[\frac{\mathbf{X}^* - E[\mathbf{X}]}{D[\mathbf{X}]} \right]} \quad (3.6-3)$$

Substitution of the design point values from Table 5.2 into Equation 3.6-3 yields a reliability index β of zero, or a probability of failure of 50% according to the standard normal cumulative distribution table. This observation is realistic since the design points were set equal to the mean values.

Now the solver function in Excel is used to solve for the design points (i.e. most likely values of the stochastic variables at failure) that will yield a limit state function of zero (i.e. failure). The solver function not only solves for the values of the design points that yield a limit state function of zero, but also minimizes the corresponding reliability index. The idea behind minimizing the reliability index is to find the set of design points that are associated with the largest probability of failure (a smaller the reliability index results in a larger the probability of failure). To reiterate, the design point values are the the most likely values at failure. Solving for the design points results in a unique reliability index for any given section modulus. The value for the section modulus is iterated until the resulting reliability index β matches the desired reliability index.

To illustrate the procedure, a few iterations of the section modulus are shown below in the following tables. Under a Poissonian assumption for a rare failure event, the

acceptable probability of failure for a 20-year lifetime is 2.0×10^{-4} which has an associated reliability index β equal to 3.54 (Ronold et al., 1999).

The first value for the section modulus is taken to be 0.007 m^3 . The results are shown in Table 5.4 (Appendix D).

Table 5.4 – First-Order Reliability Method for $W = 0.007 \text{ m}^3$

W = 0.007									
	E [X]	D [X]	X*	Z	Correlation Matrix, [R]				
log K	-12.2978	0.4810	-11.7425	1.1545	1	-0.9956	0	0	0
m	7.8794	0.2286	7.6061	-1.1957	-0.9956	1	0	0	0
e	-0.0036	0.3975	-1.3492	-3.3851	0	0	1	0	0
F_M	0.9591	0.1553	1.0445	0.5498	0	0	0	1	0
X_m	119339	82573	119339	0.0000	0	0	0	0	1

D(X)	0.9574	g(x)	0.0000	P_F	1.30E-04	β	3.65
-------------	--------	-------------	--------	----------------------	----------	----------	------

The reliability index β is calculated to be 3.65. In order to obtain a reliability index of 3.54, the section modulus needs to be decreased. A trial for $W = 0.0068 \text{ m}^3$ is shown in Table 5.5.

Table 5.5 – First-Order Reliability Method for $W = 0.0068 \text{ m}^3$

W = 0.0068									
	E [X]	D [X]	X*	Z	Correlation Matrix, [R]				
log K	-12.2978	0.4810	-11.7891	1.0576	1	-0.9956	0	0	0
m	7.8794	0.2286	7.6288	-1.0962	-0.9956	1	0	0	0
e	-0.0036	0.3975	-1.2648	-3.1727	0	0	1	0	0
F_M	0.9591	0.1553	1.0395	0.5177	0	0	0	1	0
X_m	119339	82573	119339	0.0000	0	0	0	0	1

D(X)	0.9620	g(x)	0.0000	P_F	3.18E-04	β	3.42
-------------	--------	-------------	--------	----------------------	----------	----------	------

The resulting reliability index is slightly smaller than the desired value of 3.54, hence the section modulus is increased. This procedure is continued until a final section modulus of $W = 0.006904 \text{ m}^3$ yields a reliability index of 3.54 as shown in Table 5.6.

Table 5.6 – First-Order Reliability Method for $W = 0.006904 \text{ m}^3$

W =		0.006904							
	E [X]	D [X]	X*	Z	Correlation Matrix, [R]				
log K	-12.2978	0.4810	-11.7646	1.1085	1	-0.9956	0	0	0
m	7.8794	0.2286	7.6169	-1.1484	-0.9956	1	0	0	0
e	-0.0036	0.3975	-1.3092	-3.2844	0	0	1	0	0
FM	0.9591	0.1553	1.0420	0.5335	0	0	0	1	0
Xm	119339	82573	119339	0.0000	0	0	0	0	1

D(X)	0.9597	g(x)	0.0000	PF	2.00E-04	β	3.54
-------------	--------	-------------	--------	-----------	----------	----------	------

CHAPTER 6

CALIBRATION OF PARTIAL SAFETY FACTORS

6.1 INTRODUCTION

The design ε - N curve and bending moment range (BMR) distribution are obtained by simply applying partial safety factors. The term partial safety factor is used because the overall safety factor consists of the product of the material factor γ_m and load factor γ_f .

In this chapter, first the characteristic ε - N curve is defined and then a material factor γ_m is applied in order to transform the characteristic ε - N curve into the design ε - N curve. The characteristic BMR distribution has been defined in Chapter 3 (Equation 3.3-5). This distribution is converted into an equivalent characteristic stress range (SR) distribution. A load factor γ_f is then applied in order to transform the characteristic SR distribution to the design SR distribution so as to obtain the cumulative fatigue damage to be exactly equal to one.

6.2 CHARACTERISTIC ε - N CURVE

For ε - N curves, it is standard procedure to select the characteristic ε - N curve as the ε - N curve (Equation 4.5-2)

$$\log N(S_{eq}) = E[\log K] - E[m] \log \left(\frac{S_{eq}}{2E} \right) \quad (4.5-2)$$

that is shifted to the left by two times the standard deviation of the residuals $D[e]$ (Ronold, et. al, 1999). This ε - N curve becomes the characteristic ε - N curve (Equation 6.2-1) by shifting the curve $2D[e]$ to the left and ignoring the residual term e , because it is essentially zero.

$$\log N(S_{eq}) = E[\log K] - E[m]\log\left(\frac{S_{eq}}{2E}\right) - 2D[e] \quad (6.2-1)$$

The characteristic ε - N curve is plotted as shown in Figure 6.1.

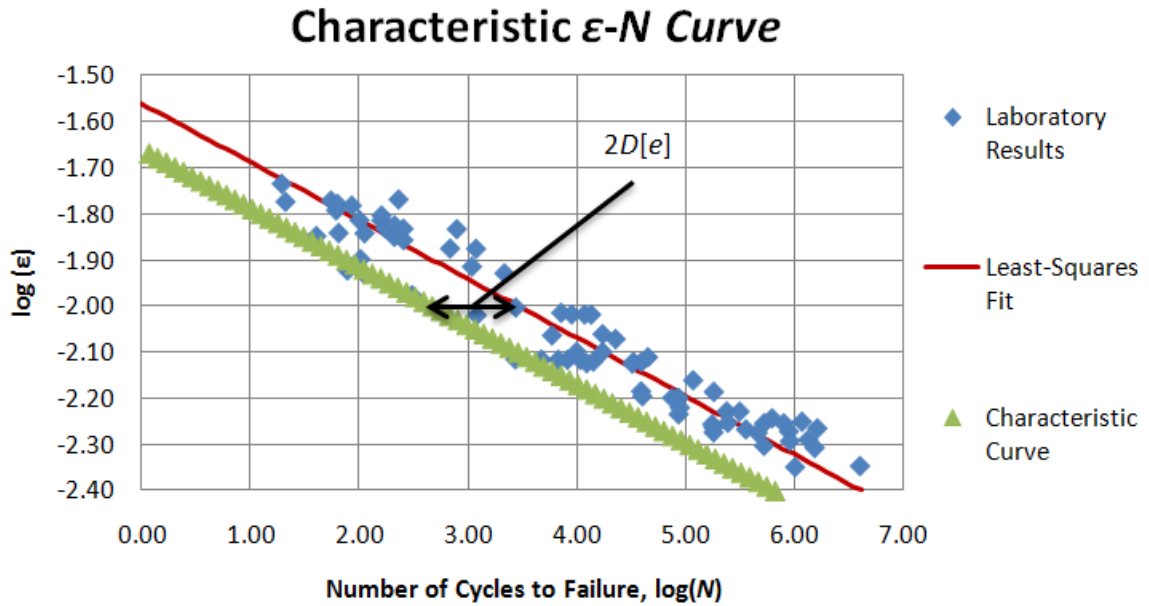


Figure 6.1 –Characteristic ε - N curve

6.3 DESIGN ε - N CURVE

A material factor γ_m is applied to the SR in Equation 6.2-1 in order to obtain the design ε - N curve as shown in Equation 6.3-1.

$$\log N(S_{eq}) = E[\log K] - E[m]\log\left(\frac{\gamma_m S_{eq}}{2E}\right) - 2D[e] \quad (6.3-1)$$

For any number of cycles to failure, the characteristic strength is divided by the material factor to obtain the design strength. Keeping in mind that the most likely values of the stochastic variables at failure are the design points \mathbf{X}^* that were calibrated in Chapter 5, the optimal material factor is one that leads to a design point ε - N curve (Equation 5.3-1, shown below)

$$\log N^*(S_{eq}) = \log K^* - m^* \log \left(\frac{S_{eq}}{2E} \right) + e^* \quad (5.3-1)$$

equal to the design ε - N curve (Equation 6.3-1). When Equations 5.3-1 and 6.3-1 are set equal to each other, an expression for the material factor is given by Equation 6.3-2.

$$\gamma_m = \frac{2E}{S} 10^{-\frac{1}{E[m]} \left(\log K^* - E[\log K] - m^* \log \left(\frac{S_{eq}}{2E} \right) + e^* + 2D[e] \right)} \quad (6.3-2)$$

The problem with this expression is that the material factor varies with different stress ranges. There needs to be a unique material factor that can be applied to all stress ranges. In order to do this, an approximation is made by assuming that the design points of the variables $\log K$ and m are set equal to the mean values calculated earlier, that is, $\log K^* = \log K$ and $m^* = m$. This yields an expression for the material factor that does not depend on the stress range and is given by.

$$\gamma_m = 10^{-\left(\frac{2D[e] + e^*}{E[m]} \right)} \quad (6.3-3)$$

where $D[e] = 0.398$ (Section 4.3.1);

$e^* = -1.0422$ (Section 5.4, Table 5.6));

$E[m] = 7.8794$ (Section 4.3.1)

Substituting the values obtained throughout the present study, the material factor is calculated to be 1.162. The design curve can be seen in Figure 6.2 below.

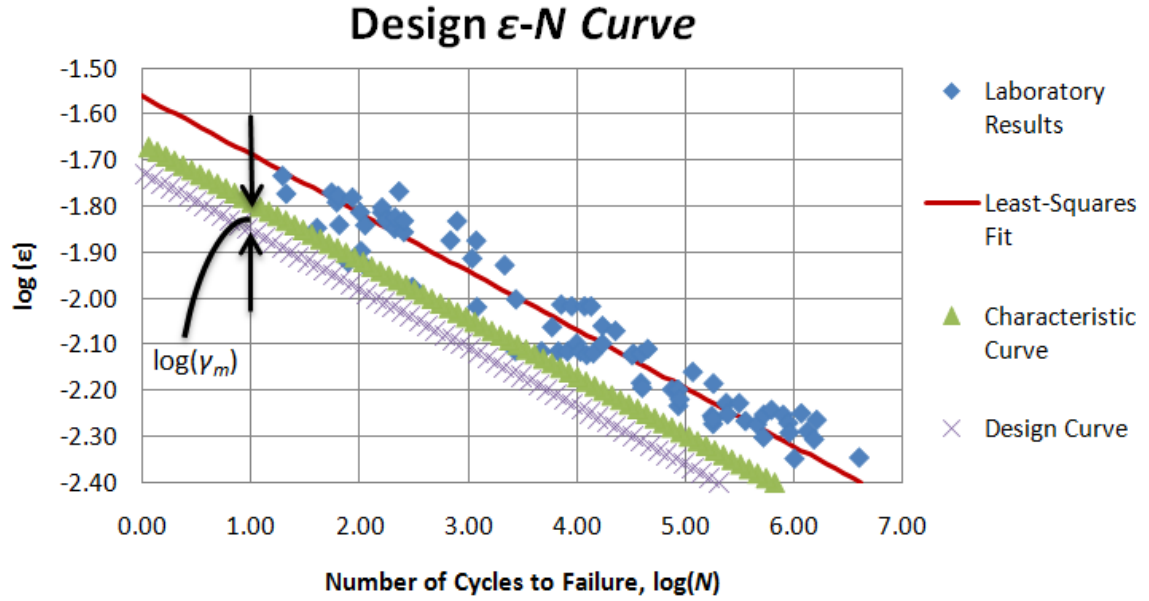


Figure 6.2 - Design ε - N curve

The material factor γ_m is applied directly to the strain and therefore, the ε - N curve is reduced in size by a factor of $\log(\gamma_m)$ as seen in Figure 6.2.

6.4 DESIGN STRESS RANGE DISTRIBUTION

The characteristic bending moment range has been defined in Chapter 4 as

$$X_i = X_a + k_R X_c \left(1 - \frac{\log(n_i)}{\log(3N_r)} \right) \quad (3.3-5)$$

which can be expressed in terms of the SR given by Equation 6.4-1.

$$S_i = \frac{X_a}{W} - \frac{k_R X_c}{W} \left(1 - \frac{\log(n_i)}{\log(3N_r)} \right) \quad (6.4-1)$$

The design SR distribution is obtained by applying a load factor γ_f to the characteristic SR distribution (Equation 6.4-1) as shown in Equation 6.4-2.

$$S_i = \gamma_f \left[\frac{X_a}{W} - \frac{k_R X_c}{W} \left(1 - \frac{\log(n_i)}{\log(3N_r)} \right) \right] \quad (6.4-2)$$

The load factor γ_f needs to be calibrated so as to predict a cumulative fatigue damage exactly equal to one when using Miner's rule (Equation 3.5-1) along with the design ε - N curve (Equation 6.3-1).

6.5 CALIBRATION OF THE LOAD FACTOR γ_F

The solver function in Microsoft Excel is used to calibrate the load factor γ_f . As a first step, Table 6.1 is developed for the computation of the cumulative fatigue damage. BMRs shown in the first column in Table 6.1 range from a maximum of 1,100 kN-m to a minimum of 485 kN-m at intervals of 2.5 kN-m. These BMR's are approximately the largest and smallest simulated BMR's from Chapter 4. In order to obtain the number of exceeding cycles in the design life n , the design SR distribution (Equation 6.4-2) is rearranged to solve directly for n .

$$n = 10^{\log(3N_r) \left[1 - \frac{W}{k_R X_c} \left(\frac{S}{\gamma_f} - \frac{X_a}{W} \right) \right]} \quad (6.5-1)$$

The number of cycles Δn for each SR interval is calculated by take the difference between two consecutive values of the number of exceeding cycles. The average SR, S_{avg} is calculated because Δn represents the number of cycles is in a SR interval; therefore the average SR of that interval is assumed to have Δn cycles. Morrow's equation (Equation 4.5-1) is used in order to determine the equivalent non-zero mean stress. The number of cycles to failure N is determined using Equation 6.3-1 and initially setting the load factor γ_f equal to one. Finally, the damage is calculated using Miner's rule (Equation 3.5-1). The solver function is now used to solve for the load factor γ_f that will yield a predicted

cumulative fatigue damage exactly equal to one.

Table 6.1 – Damage Calculations Using Design SR Distribution and Design ε - N Curve

BMR, X (N-m)	SR, S (Pa)	Number of Exceeding Cycles, n (Equation 6.5-1)	Number of Cycles in Interval, Δn	
1,100,000	1.59E+08	1.46E+05	4.85E+03	--->
1,097,500	1.59E+08	1.51E+05	5.01E+03	--->
1,095,000	1.59E+08	1.56E+05	5.18E+03	--->
.
.
.
492,500	7.13E+07	4.09E+08	1.36E+07	--->
490,000	7.10E+07	4.22E+08	1.40E+07	--->
487,500	7.06E+07	4.36E+08	1.45E+07	--->
485,000	7.02E+07	4.51E+08		
Average SR, S_{avg}	Equivalent Non-zero Mean SR, S_{eq} (Equation 4.5-1)	Number of Cycles to Failure, $\log N$ (Equation 6.3-1)	Number to Cycles to Failure, N	Damage, D (Equation 3.5-1)
1.59E+08	1.65E+08	6.66	4.56E+06	1.06E-03
1.59E+08	1.65E+08	6.67	4.64E+06	1.08E-03
1.58E+08	1.64E+08	6.67	4.72E+06	1.10E-03
.
.
.
7.11E+07	7.39E+07	9.41	2.59E+09	5.24E-03
7.08E+07	7.35E+07	9.43	2.70E+09	5.20E-03
7.04E+07	7.31E+07	9.45	2.81E+09	5.16E-03
Cumulative Fatigue Damage				1.0000

The load factor γ_f is thus calibrated to be 1.111 (Appendix E).

The material factor $\gamma_m = 1.16$ and load factor $\gamma_f = 1.11$ are very comparable to that reported in published literature (Ronold et al., 1999) where the material factor γ_m and load

factor γ_f were calculated to be 1.15 and 1.09 respectively. The design BMR distribution with a load factor $\gamma_f = 1.111$ can be seen in Figure 6.3.

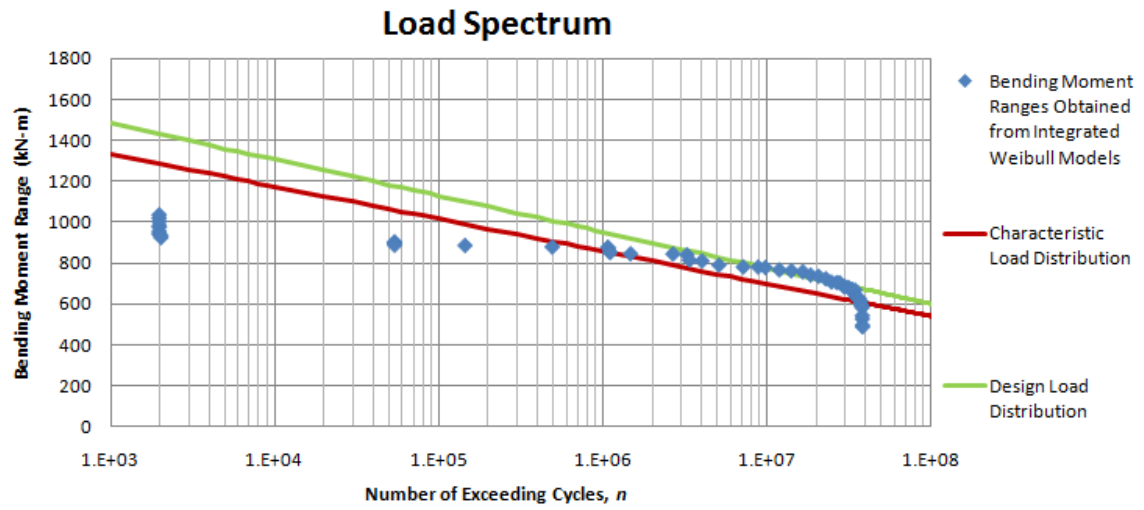


Figure 6.3 – Design BMR distribution

CHAPTER 7

SUMMARY, CONCLUSIONS, AND FUTUTRE WORK

7.1 SUMMARY

The safety of a marine current turbine (MCT) rotor blade against fatigue failure due to the computed flapwise bending moments based on site specific measured velocity is presented taking into account the inherent variability and statistical uncertainty in the load and resistance of the composite rotor blade. The load history has been modeled on the basis of simulated bending moments using blade element momentum theory at the blade root of the rotor blade subjected to currents. The resistance has been modeled in terms of an ε - N curve.

The present study also focuses on the reliability-based design of marine current turbine blades. A comprehensive review is made of existing literature regarding fatigue life predictions, reliability analysis, and partial safety factors. The loading history and material strength have been modeled and the statistical uncertainties of the modeling have been taken into consideration in the reliability analysis. A reliability based calibration of partial safety factors has been performed for the rotor blade against fatigue failure in flapwise bending. The material factor γ_m and load factor γ_f were determined to be 1.16 and 1.11 respectively, which compare well with the published data on wind turbine rotor blades (Ronold et al., 1999).

7.2 CONCLUSIONS

The cumulative damage leading to a fatigue failure has been predicted based on Miner's sum formulation. The models for load, resistance, and cumulative damage in an ocean current turbine rotor blade are used in defining a limit state function for fatigue failure. The uncertainty in the residuals of the ε - N curve is identified as an important uncertainty source. The following conclusions are made based on the limited study and the numerical simulation:

- i. The short-term distribution of the out-of-plane (flapwise) bending moments in a full-scale polyester reinforced laminate rotor blade can be used to represent the long-term distribution in a MCT.
- ii. The long-term distribution of flapwise bending moments can be effectively modeled based on the 2-parameter Weibull model.
- iii. The effect of non-zero mean stress in the fatigue damage calculations contributes to about 54% more damage compared to that based on assuming a zero mean stress.
- iv. The probabilistic based fatigue life MCT rotor blades can be predicted using Miner's rule from the existing laboratory test data for polyester laminates represented by the ε - N curve.
- v. Major uncertainty sources associated with load and resistance can be included in the reliability analysis through calibration of a load factor and a material factor for use in design.

7.3 FUTURE WORK

The following additional uncertainty sources associated with the Miner's sum formulation in the prediction of cumulative damage of MCT rotor blades need to be considered:

- i. size effects in material properties
- ii. temperature dependencies
- iii. special lamination problems near the rotor blade root
- iv. long-term environmental degradation effects due to material wear and exposure to sea water.

Also, the nonlinear relationship between stress and strain, especially in the high stress range needs further study.

Future work is suggested to investigate a series of MCT rotor blades with different composite material properties that are located at different sites with the ultimate goal of developing a reliability-based optimal design code. Other suggestions are to investigate the fatigue due to edgewise bending as well as fatigue of other MCT composites.

APPENDIX A - Procedure

Loading

1. Select the location.
2. Measure the wave current velocities in 30 minute intervals for a period of one month.
3. Generate the bending moment time history (30-minute time history) for each measured velocity using MathCAD.
4. Extract peaks (maximum) and valleys (minimums) from the 30-minute bending moment time histories.
5. Discretize the one month period of wave current velocities into 8 hour records
6. For each 8-hour record:
 - a. Calculate the mean current velocity and turbulence intensity.
 - b. Assemble the 30-minute bending moment time histories in order according to the 16 wave currents that make up the 8-hour record.
 - c. Rainflow count the bending moment time history to obtain the bending moment ranges, X .
 - d. Calculate the mean and standard deviation of the bending moments.
7. Select bin sizes based upon mean current velocities and turbulence intensities calculated for each 8-hour record.
8. Sort 8-hour records into appropriate bins according the 8-hour record's mean current velocity and turbulence intensity
9. For each bin:
 - a. Arrange the bending moment ranges (BMRs) in ascending order.
 - b. Solve for constants a and b using Matlab in order to fit the Weibull distribution to the simulated BMRs.
 - c. Discretize the Weibull fit into number the same number of 8-hour intervals that make up the bin.
 - d. Plug in the constants a and b to the CDF to obtain the cumulative probability at each boundary of the interval.
 - e. Calculate probability content of each interval by subtraction.
 - f. Multiply the probability content and total number of cycles in the bin to obtain the number of cycles within each interval (use average value of bending moment range to obtain pairs of $X-n$)
10. Integrate all pairs of $X-n$ from all bins.

11. Select a design life and multiply number of occurrences by 12*design life (in years).
12. Sort BMRs in descending order and count total number of cycles (number of exceeding cycles: i.e. number of cycles occurring at a given bending moment range or higher).
13. Plot load spectrum (bending moment range vs. number of exceeding cycles).
14. Fit characteristic BMR distribution to load integrated Weibull model distribution.

Resistance

1. Select a material
2. Run ε - N tests to obtain pairs of strain and number of cycles to failure
3. Calculate the mean, standard deviation, and correlation coefficient of $\log K$ and m .
4. Calculate the mean and standard deviation of e .
5. Use linear regression to fit the ε - N data.

Damage

1. For each bin:
 - a. Calculate the damage $D(x)$ based on simulated BMRs.
 - b. Calculate the damage $D(x)$ based on the integrated on Weibull fits.
 - c. Calculate ratio of damage, F_M , calculated from empirical data to damage cause by model.
2. Calculate $E[F_M]$ and $D[F_M]$.

Reliability Analysis (uses integration of Weibull models for the loading history)

1. Construct a table with the mean, standard deviation, design points* (currently unknown – for now, set = to mean values) and the correlation matrix of the variables $\log K$, m , e , F_M , and X_m .
2. Calculate Z-values for each variable.
3. Select a section modulus W ($S = X/W$ and $S = 2E\varepsilon \rightarrow \varepsilon = X/(2EW)$).
4. Calculate the design points that will yield a limit state function $g(x) = 1 - F_M D(x)$ equal to zero while minimizing the reliability index β .
5. Iterate the value of the section modulus until desired reliability index is reached.

Calibration of Partial Safety Factors

1. Calculate the material factor γ_m based upon e^* , $2\sigma_e$, and $E[m]$ (setting design point ε - N curve equal to the design ε - N curve).
2. Apply a random load factor γ_f to the characteristic load distribution.
3. Calibrate the load factor that yields a damage $D(x) = 1.0$.

APPENDIX B

i. MATLAB code for obtaining peaks and valleys for rainflow counting method

```
clc
clear all

x = [data];

L = length(x); % Count number of bending moment range values

% Find Maximum Points

X=zeros(L,1); % Column matrix - all zeros
for i = 7:L-1
    if (x(i)>=x(i-1) & x(i)>=x(i-2) & x(i)>=x(i-3) & x(i)>=x(i-4) & x(i)>=x(i-5) & x(i)>=x(i-6) & x(i)>=x(i-7) & x(i)>=x(i-8) & x(i)>=x(i-10) & x(i)>x(i+1))
        X(i) = x(i); % Locate when one bending moment is greater than or equal to the previous bending moment(s), aka the peaks (multiple times in case there are several maximum values that are equal)
    end
end
X(X==0) = []; % Delete zeros leaving only the maximum values in the X column matrix
X=[x(1);X]; % Bring in 1st maximum point

% Finding Minimum Points

y=-x; % Negate all values of bending moments
Y=zeros(L,1); % Column matrix - all zeros
for i = 11:L-1
    if (y(i)>=y(i-1) & y(i)>=y(i-2) & y(i)>=y(i-3) & y(i)>=y(i-4) & y(i)>=y(i-5) & y(i)>=y(i-6) & y(i)>=y(i-7) & y(i)>=y(i-8) & y(i)>=y(i-9) & y(i)>=y(i-10) & y(i)>y(i+1))
        Y(i) = y(i); % Locate when one bending moment is greater than or equal to the previous bending moment(s), aka the peaks (multiple times in case there are several minimum values that are equal)
    end
end
Y(Y==0) = []; % Delete zeros leaving only the minimum values in the Y matrix
Y=-Y; % Negate all values in order to obtain original bending moments (because they were previously negated)

% Combine X (maximum) and Y (minimum) column matrices into one matrix

LX = length(X); % Calculate new length of X (maximum) column matrix now that zeros have been deleted
```

```

LY = length(Y); % Calculate new length of Y (minimum) column matrix now that zeros have been deleted
Z = zeros(LX+LY,1); % Create a zero column matrix (Z) the length of both X (maximum) and Y
(minimum) column matrices combined
for i = 1:LY
    Z(2*i) = X(i); % Place maximum values into every other position of the Z column matrix starting with
the 2nd value
    Z(2*i+1) = Y(i); % Place minimum values into every other position of the Z column matrix starting with
the 3rd value
end
Z(Z==0) = [] % Delete 1st zero
Z = [Z;X(LX)] % Copy 1st value (which is a maximum) and place it at the end of the Z column matrix
(needed for rainflow counting program)
plot(Z)
grid on

```

ii. MATLAB code for rainflow counting method

```
clc
clear all

% Database of bending moments (no values below u150 (u = 1.50 m/s) because rotor blades stalled)

u0 = [u0data];
.
.
.
u203 = [u203data];

% Data (Three 8 hour records ped day for a month)
y1 = [u157,u167,u170,u165,u167,u168,u166,u172,u175,u166,u173,u173,u179,u183,u178,u172,];
y2 = [u172,u176,u173,u174,u177,u179,u174,u181,u180,u179,u178,u176,u175,u187,u189,u187,];
y3 = [u191,u189,u188,u190,u188,u189,u187,u188,u182,u185,u188,u183,u186,u186,u184,u183,];
y5 = [u185,u170,u187,u183,u182,u180,u166,u177,u145,u128,u140,u119,u105,u134,u120,u112,];
y7 = [u192,u185,u181,u178,u184,u199,u200,u193,u191,u167,u126,u186,u170,u166,u188,u186,];
y8 = [u182,u176,u171,u171,u174,u166,u162,u167,u158,u143,u149,u162,u155,u117,u130,u167,];
y11 = [u162,u129,u192,u194,u192,u194,u185,u183,u179,u174,u177,u172,u176,u176,u178,u177,];
y12 = [u177,u183,u180,u184,u181,u182,u181,u182,u186,u186,u189,u177,u191,u192,u183,u187,];
y13 = [u188,u181,u183,u189,u189,u196,u192,u195,u188,u199,u196,u194,u198,u202,u196,u191,];
y14 = [u186,u182,u177,u179,u174,u176,u171,u171,u165,u163,u159,u162,u160,u161,u159,u152,];
y15 = [u151,u156,u158,u159,u163,u161,u166,u161,u169,u171,u170,u172,u176,u179,u178,u180,];
y16 = [u177,u159,u164,u163,u163,u157,u175,u166,u167,u165,u169,u172,u169,u159,u159,u148,];
y17 = [u140,u164,u161,u167,u164,u171,u172,u172,u176,u175,u174,u170,u169,u156,u164,u160,];
y18 = [u162,u164,u158,u154,u158,u152,u157,u163,u167,u171,u165,u169,u160,u165,u171,u173,];
y19 = [u175,u178,u171,u170,u175,u163,u171,u159,u159,u172,u177,u186,u159,u115,u125,u143,];
y21 = [u146,u150,u156,u153,u155,u151,u154,u159,u165,u161,u164,u156,u134,u168,u175,u175,];
y22 = [u177,u180,u182,u178,u181,u169,u172,u176,u176,u183,u181,u180,u181,u185,u161,u143,];
y23 = [u172,u172,u156,u178,u153,u165,u158,u111,u175,u155,u131,u170,u174,u177,u175,u172,];
y24 = [u161,u159,u160,u160,u159,u162,u164,u163,u168,u164,u164,u173,u170,u172,u173,u173,];
y25 = [u174,u160,u165,u166,u165,u163,u159,u166,u165,u170,u174,u169,u175,u178,u183,u180,];
y27 = [u166,u167,u173,u165,u163,u159,u135,u112,u96,u128,u152,u166,u167,u168,u168,u165,];
y28 = [u176,u177,u177,u177,u172,u170,u170,u163,u159,u160,u158,u165,u164,u167,u175,u177,];
y29 = [u183,u185,u187,u192,u191,u193,u194,u147,u188,u165,u192,u188,u173,u181,u185,u183,];
y30 = [u183,u172,u168,u163,u162,u156,u156,u162,u165,u164,u178,u174,u172,u171,u181,u171,];
y31 = [u180,u200,u202,u156,u195,u196,u198,u193,u193,u185,u188,u186,u185,u188,u181,u176,];
y35 = [u145,u141,u163,u165,u175,u170,u172,u170,u178,u177,u186,u185,u195,u194,u197,u191,];
y36 = [u189,u180,u180,u189,u188,u183,u179,u170,u158,u148,u141,u149,u155,u168,u168,u165,];
y38 = [u156,u147,u146,u153,u157,u165,u169,u167,u168,u167,u178,u177,u180,u184,u182,u186,];
y39 = [u181,u181,u179,u167,u169,u166,u162,u165,u165,u161,u155,u159,u156,u166,u157,u163,];
y40 = [u164,u164,u163,u167,u165,u161,u166,u162,u167,u167,u166,u168,u169,u163,u165,u159,];
y42 = [u150,u160,u153,u171,u157,u154,u154,u152,u155,u161,u163,u156,u150,u152,u134,u153,];
y43 = [u160,u156,u159,u166,u168,u175,u176,u177,u183,u183,u188,u179,u185,u189,u188,u192,];
y44 = [u193,u191,u199,u201,u203,u200,u194,u193,u191,u197,u192,u191,u191,u181,u180,u181,];
y45 = [u176,u167,u168,u169,u170,u160,u165,u162,u162,u157,u149,u152,u143,u148,u151,u161,];
y46 = [u160,u164,u165,u162,u157,u164,u158,u162,u157,u153,u150,u149,u157,u157,u152,u156,];
y48 = [u146,u143,u149,u152,u148,u160,u155,u151,u152,u153,u153,u152,u153,u155,u158,u157,];
y49 = [u161,u163,u166,u166,u171,u169,u173,u163,u162,u156,u156,u160,u150,u150,u146,u145,];
```



```

y51 = [u150,u152,u153,u154,u151,u154,u155,u153,u156,u152,u153,u148,u150,u149,u150,u152,];
y52 = [u155,u156,u154,u157,u164,u161,u161,u171,u161,u171,u172,u170,u171,u170,u161,u171,];
y55 = [u27,u153,u159,u149,u153,u158,u160,u162,u167,u158,u165,u162,u169,u171,u167,u166,];
y56 = [u171,u166,u166,u169,u166,u163,u168,u167,u169,u164,u162,u163,u158,u160,u162,u161,];
y57 = [u163,u156,u156,u158,u162,u147,u161,u173,u168,u167,u163,u172,u176,u177,u182,u183,];
y58 = [u185,u183,u189,u194,u199,u195,u190,u189,u197,u200,u196,u190,u190,u193,u190,u179,];
y59 = [u171,u175,u167,u168,u163,u164,u151,u152,u147,u138,u144,u136,u138,u136,u130,u137,];
y62 = [u151,u153,u149,u152,u154,u153,u151,u151,u153,u153,u152,u151,u151,u148,u149,u152,];
y63 = [u147,u146,u145,u146,u151,u151,u155,u157,u158,u158,u157,u155,u157,u160,u158,u156,];
y64 = [u154,u151,u155,u153,u152,u152,u153,u158,u153,u160,u161,u160,u156,u158,u154,u159,];
y72 = [u156,u156,u153,u156,u154,u156,u160,u158,u162,u157,u152,u142,u148,u148,u151,u147,];
y78 = [u147,u145,u145,u145,u148,u150,u150,u155,u156,u161,u164,u171,u177,u177,u177,u176,];
y85 = [u147,u152,u162,u158,u161,u156,u159,u157,u148,u142,u146,u145,u144,u146,u146,u150,];
y86 = [u151,u148,u145,u148,u153,u154,u153,u154,u158,u156,u161,u156,u163,u164,u168,u168,];
y87 = [u161,u167,u168,u165,u170,u168,u163,u167,u164,u167,u168,u171,u168,u171,u178,u177,];
y88 = [u176,u183,u182,u190,u180,u188,u184,u188,u181,u187,u188,u181,u182,u176,u178,u174,];
y89 = [u171,u173,u173,u169,u172,u173,u172,u174,u174,u174,u168,u174,u179,u172,u178,u180,];
y90 = [u179,u177,u180,u176,u178,u171,u171,u173,u181,u180,u179,u174,u180,u176,u181,u181,];
y91 = [u188,u198,u193,u196,u194,u199,u202,u195,u199,u197,u191,u195,u185,u184,u184,u177,];
y92 = [u168,u163,u161,u164,u167,u158,u154,u150,u149,u157,u156,u149,u150,u150,u151,u150,];

```

`x = y1; % Change this value in order to obtain the rainflow counting results for the given record number`

```

[C,I] = max(x); % Locate largest peak
x = [x(I:end) x(1:I-1) C]'; % Rearrange original data so vector begins with largest peak (also adding one
more value (largest peak) at end)
t=linspace(0,8,length(x))'; % Create a time vector (8-hours)
plot(t,x./1000)
title('Bending Moment Ranges for Record #85')
xlabel('Time (hours)')
ylabel('Bending Moment (kNm)')

```

```

p = 1; % Start with the 1st x
q = length(x)-1; % Number of elements in x minus 1 (minus 1 b/c x(p+1))
H = zeros(2,length(x/2-1)); % Creating empty matrix to place deleted information into. 2 rows by
length(x)-1 columns. Each new column represents the set of x's being deleted

```

`n = 0; % n represents the column number of the empty matrix (zero b/c $n = n + 1 = 0 + 1 = 1$)`

```

while p<=q % Loop from p to q
    r(1) = abs(x(p)-x(p+1)); % Calculate 1st range (to be compared w/ 2nd)
    r(2) = abs(x(p+1)-x(p+2)); % Calculate 2nd range (to be compared w/ 1st)
    if r(1)<=r(2) % If 1st range is <= to 2nd range
        n = n + 1; % Place next set of deleted x's into next column
        H(:,n) = x(p:p+1); % Filling in x's that are about to be deleted into the nth column
        x(p) = []; % Erase 1st x value
        x(p+1) = []; % Erase 2nd x value
        q = length(x)-2; % Recalculate the number of x's (minus 2 b/c 2 x's were deleted)
        p = 1; % Start the loop from the beginning
    else
        p = p + 1; % Check the next two sets of r's
    end
end

```

```
H = H(:,1:n); % Display entire matrix( : means fill in all rows) (1:n means fill in columns 1 through n)
mn = mean(H)'; % Calculate the mean of each set of x's
rng = abs(diff(H))'; % Calculate the range of each set of x's
mean(mn) % Calculate the mean 8-hour current velocity E[U_8]
```

APPENDIX C

i. Microsoft Excel code for cumulative probability calculations (Table 4.1)

a. example

	A	B	C	D	E	F	G	H
1	sum n		X	ln(X)	n	Cumulative n	F(x)	ln(-ln(1-F(x)))
2	15345		499000	13.12	1	1	4.56E-05	-10.00
3			507000	13.14	1	2	1.11E-04	-9.11
4			581000	13.27	1	3	1.76E-04	-8.65

b. code

	C	D	E	F	G	H
1	X	ln(X)	n	Cumulative n	F(x)	ln(-ln(1-F(x)))
2	499000	=LN(C2)	1	=E2	=(F2-0.3)/(\$A\$2+0.4)	=LN(-LN(1-G2))
3	507000	=LN(C3)	1	=F2+E3	=(F3-0.3)/(\$A\$2+0.4)	=LN(-LN(1-G3))
4	581000	=LN(C4)	1	=F3+E4	=(F4-0.3)/(\$A\$2+0.4)	=LN(-LN(1-G4))

ii. Microsoft Excel code for calculation of number of exceeding cycles in design life (Table 4.4)

a. example

	A	B	C	D	E	F	G
1	design life		Compound Weibull Model Loading History				
2	20		X (N-m)	X (kN-m)	n	n.e	design life n
3			1.037E+06	1037	8.27	8.3	1.98E+03
4			1.021E+06	1021	0.00	8.3	1.98E+03
5			1.004E+06	1004	0.00	8.3	1.99E+03

b. code

The BMRs from each bin are copied and pasted in one column manually and then sorted from largest to smallest using the “Sort & Filter” command. The results are shown in column C.

	C	D	E	F	G
1	Compound Weibull Model Loading History				
2	X (N-m)	X (kN-m)	n	n.e	design life n
3	1037150	=C3/1000	8.26848258482848	=E3	=F3*\$A\$2*12
4	1021000	=C4/1000	0	=F3+E4	=F4*\$A\$2*12
5	1004075	=C5/1000	0.00476539239855356	=F4+E5	=F5*\$A\$2*12

iii. MATLAB code for least-squares regression of ε - N data and mean, standard deviation, and correlation coefficient of $\log K$ and m (Section 4.3)

```
clc
clear all

data = [1.29    -1.74
1.32    -1.77
1.61    -1.85
1.74    -1.77
1.79    -1.79
1.80    -1.78
1.81    -1.84
1.89    -1.92
1.93    -1.78
2.00    -1.81
2.01    -1.90
2.04    -1.93
2.05    -1.84
2.20    -1.81
2.20    -1.80
2.24    -1.83
2.32    -1.85
2.32    -1.83
2.36    -1.77
2.40    -1.86
2.41    -1.83
2.48    -1.98
2.83    -1.88
2.89    -1.83
3.03    -1.91
3.07    -1.88
3.08    -2.02
3.33    -1.93
3.43    -2.12
3.44    -2.00
3.67    -2.12
3.77    -2.06
3.83    -2.12
3.85    -2.01
3.91    -2.12
3.95    -2.02
3.99    -2.10
4.03    -2.12
4.07    -2.02
4.09    -2.12
4.13    -2.02
4.15    -2.12
4.23    -2.10
4.23    -2.06
4.35    -2.07
4.51    -2.12
4.52    -2.12
4.59    -2.18
4.59    -2.12]
```

```

4.60      -2.20
4.65      -2.11
4.87      -2.20
4.92      -2.20
4.93      -2.23
4.93      -2.20
4.94      -2.22
5.06      -2.16
5.24      -2.26
5.25      -2.27
5.25      -2.26
5.25      -2.19
5.37      -2.23
5.38      -2.25
5.49      -2.23
5.55      -2.27
5.66      -2.27
5.72      -2.30
5.72      -2.25
5.79      -2.24
5.90      -2.25
5.94      -2.27
5.95      -2.29
6.00      -2.35
6.06      -2.25
6.12      -2.29
6.18      -2.31
6.21      -2.27
6.60      -2.35];

```

```

logN = data(:,1);
logepsilon = data(:,2);

```

```

x = logN;
y = logepsilon;
L = length(x);

```

```

l = linspace(1,1,L)';
A = [l -logepsilon];
coeff = A\logN(:);
logK = coeff(1);
m = coeff(2);
F = [logK, m]'

```

```

logN = logK - m.*logepsilon;

```

```

plot(x,y,'x',logN,logepsilon)
xlim([0,7])
ylim([-2.4,-1.4])
xlabel('log N')
ylabel('log epsilon')
title('Laboratory Results from Composite')
a=x';
b=y';

```

```

a = ones(L,1)*a;
a(eye(L)==1) = [];
a = reshape(a',L,L-1);

b = ones(L,1)*b;
b(eye(L)==1) = [];
b = reshape(b',L,L-1);
a=a';
b=b';

l2 = linspace(1,1,L-1)';
C = zeros(L,2);

for i = 1:L
    B = [l2 -b(:,i)];
    coeff = B\a(:,i);
    logK = coeff(1);
    m = coeff(2);
    C(i,1) = logK;
    C(i,2) = m;
end

for i = 1:L
    slogK(i) = (C(i,1) - mean(C(:,1))).^2; % (a-average(a))^2
end

for i = 1:L
    sm(i) = (C(i,2) - mean(C(:,2))).^2; % (a-average(a))^2
end

SlogK = sum(slogK); % summing up all s1'a
Sm = sum(sm);
S = [SlogK,Sm]';

DlogK = sqrt((L-1)*SlogK/L); % std. dev of mean values
Dm = sqrt((L-1)*Sm/L); % std. dev of std. dev. values
D = [DlogK,Dm]' % matrix of std. dev. of 1st 3 moments
for i = 1:L
    slogK2(i) = (C(i,1) - mean(C(:,1))).^2; % (a-average(a))^2
end

for i = 1:L
    sm2(i) = (C(i,2) - mean(C(:,2))).^2; % (a-average(a))^2
end

row = (L-1)./L*sum((slogK2.*sm2)./(DlogK.*Dm))

```

iv. Microsoft Excel code for fatigue damage calculations based on simulated BMRs (Table 4.6)

a. example

	A	B	C	D	E	F	G	H
1	<i>W</i>	0.007		<i>X (N-m)</i>	<i>SR</i>	<i>n</i>	<i>N</i>	<i>D</i>
2	<i>log K</i>	-12.2978		499000	71285714	1	5.20E+10	1.92E-11
3	<i>m</i>	7.8794		507000	72428571	1	4.59E+10	2.18E-11
4	<i>E</i>	2.97E+10		581000	83000000	1	1.57E+10	6.37E-11
5	<i>D</i>	5.72E-06		585000	83571429	1	1.49E+10	6.73E-11

b. code

	A	B	C	D	E	F	G	H
1	<i>W</i>	0.007		<i>X (N-m)</i>	<i>SR</i>	<i>n</i>	<i>N</i>	<i>D</i>
2	<i>log K</i>	='[Last Thesis (Appen		499000	=D2/\$B\$1	1	=10^(\$B\$2-\$B\$3*LOG(E2/(2*\$B\$4)))	=F2/G2
3	<i>m</i>	='[Last Thesis (Appen		507000	=D3/\$B\$1	1	=10^(\$B\$2-\$B\$3*LOG(E3/(2*\$B\$4)))	=F3/G3
4	<i>E</i>	29700000000		581000	=D4/\$B\$1	1	=10^(\$B\$2-\$B\$3*LOG(E4/(2*\$B\$4)))	=F4/G4
5	<i>D</i>	=SUM(H2:H15376)		585000	=D5/\$B\$1	1	=10^(\$B\$2-\$B\$3*LOG(E5/(2*\$B\$4)))	=F5/G5

v. Microsoft Excel code for fatigue damage calculations based on Weibull model (Table 4.7)

a. example

	A	B
1	W	0.007
2	log K	-12.2978
3	m	7.8794
4	E	2.97E+10
5	# of cycles in bin	15375
6		
7	<u>Weibull Constants</u>	
8	a	737879
9	b	14.9799

	D	E	F	G	H	I	J	K	L
1	X	Cum. Prob.	Interval	X (average)	SR	Prob. Content	n	N	D
2	499000	0.00	1	540500	7.72E+07	0.025	389.49	2.77E+10	1.40E-08
3	582000	0.03	2	623500	8.91E+07	0.162	2486.45	9.00E+09	2.76E-07
4	665000	0.19	3	706500	1.01E+08	0.517	7945.02	3.36E+09	2.36E-06
5	748000	0.71	4	789500	1.13E+08	0.291	4469.47	1.40E+09	3.19E-06
6	831000	1.00	5	872500	1.25E+08	0.003	40.79	6.37E+08	6.40E-08
7	914000	1.00	6	955500	1.37E+08	0.000	0.00	3.11E+08	9.34E-16
8	997000	1.00						Cum. D	5.91E-06

b. code

	D	E	F	G	H
1	X	Cum. Prob.	Interval	X (average)	SR
2	499000	=1-EXP(-((D2/B\$8)^B\$9))	1	=AVERAGE(D2:D3)	=G2/\$B\$1
3	582000	=1-EXP(-((D3/B\$8)^B\$9))	2	=AVERAGE(D3:D4)	=G3/\$B\$1
4	665000	=1-EXP(-((D4/B\$8)^B\$9))	3	=AVERAGE(D4:D5)	=G4/\$B\$1
5	748000	=1-EXP(-((D5/B\$8)^B\$9))	4	=AVERAGE(D5:D6)	=G5/\$B\$1
6	831000	=1-EXP(-((D6/B\$8)^B\$9))	5	=AVERAGE(D6:D7)	=G6/\$B\$1
7	914000	=1-EXP(-((D7/B\$8)^B\$9))	6	=AVERAGE(D7:D8)	=G7/\$B\$1
8	997000	=1-EXP(-((D8/B\$8)^B\$9))			

	I	J	K	L
1	Prob. Content	n	N	D
2	=E3-E2	=I2*\$B\$5	=10^(\$B\$2-\$B\$3*LOG(H2/(2*\$B\$4)))	=J2/K2
3	=E4-E3	=I3*\$B\$5	=10^(\$B\$2-\$B\$3*LOG(H3/(2*\$B\$4)))	=J3/K3
4	=E5-E4	=I4*\$B\$5	=10^(\$B\$2-\$B\$3*LOG(H4/(2*\$B\$4)))	=J4/K4
5	=E6-E5	=I5*\$B\$5	=10^(\$B\$2-\$B\$3*LOG(H5/(2*\$B\$4)))	=J5/K5
6	=E7-E6	=I6*\$B\$5	=10^(\$B\$2-\$B\$3*LOG(H6/(2*\$B\$4)))	=J6/K6
7	=E8-E7	=I7*\$B\$5	=10^(\$B\$2-\$B\$3*LOG(H7/(2*\$B\$4)))	=J7/K7
8			Cum. D	=SUM(L2:L7)

vi. Microsoft Excel code for fatigue damage calculation accounting for non-zero mean stresses (Table 4.8)

a. example

	A	B
1	design life	20
2	log K	-12.2978
3	m	7.8794
4	E	2.97E+10
5	W	0.007
6	X.m	3.22E+08
7	X.o	1.19E+05
8	S.o	1.70E+07
9		
10	Damage	0.02798

	D	E	F	G	H	I	J
1	X (N-m)	S (Pa)	S.eq	n	Design life n	N	D
2	1.037E+06	1.482E+08	1.564E+08	8.27	1.984E+03	1.063E+08	1.867E-05
3	1.021E+06	1.459E+08	1.540E+08	0.00	0.000E+00	1.203E+08	0.000E+00
4	1.004E+06	1.434E+08	1.515E+08	0.00	1.144E+00	1.372E+08	8.336E-09

b. code

	A	B
1	design life	20
2	log K	-12.2978
3	m	7.8794
4	E	29700000000
5	W	0.007
6	X.m	322000000
7	X.o	119338.947368421
8	S.o	=B7/B5
9		
10	Damage	=SUM(J2:J56)

	D	E	F	G	H	I	J
1	X (N-m)	S (Pa)	S.eq	n	Design life n	N	D
2	1037150	=D2/\$B\$5	=E2/(1-\$B\$8/\$B\$6)	8.268482	=G2*\$B\$1*12	=10^(\$B\$2-\$B\$3*LOG(F2/(2*\$B\$4)))	=H2/I2
3	1021000	=D3/\$B\$5	=E3/(1-\$B\$8/\$B\$6)	0	=G3*\$B\$1*12	=10^(\$B\$2-\$B\$3*LOG(F3/(2*\$B\$4)))	=H3/I3
4	1004075	=D4/\$B\$5	=E4/(1-\$B\$8/\$B\$6)	0.004765	=G4*\$B\$1*12	=10^(\$B\$2-\$B\$3*LOG(F4/(2*\$B\$4)))	=H4/I4

vii. Microsoft Excel code for fatigue damage calculations using the characteristic BMR distribution (Table 4.9)

a. example

	A	B	C	D
1	design life	T.L	20	years
2		log K	-12.2978	
3		m	7.8794	
4	Young's modulus	E	2.97E+10	Pa
5	section modulus	W	0.007	m ³
6	static strength	S.o	3.22E+08	Pa
7	mean BMR	X.m	1.19E+05	N-m
8	mean SR	S.m	1.70E+07	Pa
9				
10	current velocity a	v.o	1.5	m/s
11	length of rotor blade	R	10	m
12	frequency	f.r	7	rpm
13		=	0.12	s ⁻¹
14		w ²	26.13	m ² /s ²
15	density	ρ	1000	kg/m ³
16	characteristic chord	c	1.685	m
17	lift coefficient	C.L	1.28	
18		X.c	939358	kg m ² /s ²
19	scaling factor	k.R	1.409	
20	number of rotations	N.r	7.36E+07	rotations
21	Adjustment	X.a	485750	N-m
22		S.a	6.94E+07	Pa
23				
24	Damage	D	0.02798	

	G	H	I	J	K	L	M
1	n	Δn	X (N-m)	Avg. S (Pa)	S.eq (Pa)	N	D
2	1.00E+01	1.00E+01	1.651E+06	2.324E+08	2.454E+08	3.058E+06	3.271E-06
3	2.00E+01	1.00E+01	1.603E+06	2.270E+08	2.397E+08	3.681E+06	2.717E-06
4	3.00E+01	1.00E+01	1.575E+06	2.236E+08	2.361E+08	4.147E+06	2.411E-06
5	4.00E+01	1.00E+01	1.556E+06	2.211E+08	2.335E+08	4.533E+06	2.206E-06

b. code

	A	B	C	D
1	design life	T.L	20	years
2		log K	-12.2978	
3		m	7.8794	
4	Young's modulus	E	29700000000	Pa
5	section modulus	W	0.007	m ³
6	static strength	S.o	322000000	Pa
7	mean BMR	X.m	119338.947368421	N-m
8	mean SR	S.m	=C7/C5	Pa
9				
10	current velocity at stalling	v.o	1.5	m/s
11	length of rotor blade	R	10	m
12	frequency	f.r	7	rpm
13		=	=C12/60	s ⁻¹
14		w ²	=(4*PI()/3*C13*C11)^2+C10^2	m ² /s ²
15	density	ρ	1000	kg/m ³
16	characteristic chort length at 2R/3	c	1.685	m
17	lift coefficient	C.L	1.28	
18		X.c	=C15/2*C14*C16*C17*C11^2/3	kg m ² /s ²
19	scaling factor	k.R	1.4094134771379	
20	number of rotations in design life	N.r	=C13*3600*24*365.25*C1	rotations
21	Adjustment	X.a	485750	N-m
22		S.a	=C21/\$C\$5	Pa
23				
24	Damage	D	=SUM(M2:M248)	

	G	H	I
1	n	Δn	X (N-m)
2	10	=G3-G2	=\$C\$21+\$C\$19*\$C\$18*(1-LOG(G2)/(LOG(3*\$C\$20)))
3	20	=G4-G3	=\$C\$21+\$C\$19*\$C\$18*(1-LOG(G3)/(LOG(3*\$C\$20)))
4	30	=G5-G4	=\$C\$21+\$C\$19*\$C\$18*(1-LOG(G4)/(LOG(3*\$C\$20)))
5	40	=G6-G5	=\$C\$21+\$C\$19*\$C\$18*(1-LOG(G5)/(LOG(3*\$C\$20)))

	J	K	L	M
1	Avg. S (Pa)	S.eq (Pa)	N	D
2	=AVERAGE(I2:I3)/\$C\$5	=J2/(1-\$C\$8/\$C\$6)	=10^(\$C\$2-\$C\$3*LOG(K2/(2*\$C\$4)))	=H2/L2
3	=AVERAGE(I3:I4)/\$C\$5	=J3/(1-\$C\$8/\$C\$6)	=10^(\$C\$2-\$C\$3*LOG(K3/(2*\$C\$4)))	=H3/L3
4	=AVERAGE(I4:I5)/\$C\$5	=J4/(1-\$C\$8/\$C\$6)	=10^(\$C\$2-\$C\$3*LOG(K4/(2*\$C\$4)))	=H4/L4
5	=AVERAGE(I5:I6)/\$C\$5	=J5/(1-\$C\$8/\$C\$6)	=10^(\$C\$2-\$C\$3*LOG(K5/(2*\$C\$4)))	=H5/L5

APPENDIX D

i. Microsoft Excel code for damage calculations using the design point ε - N curve (Table 5.3)

a. example

	A	B	C	D	E	F	G	H	I
1	$\log K^*$	-12.2978		X (N-m)	S (Pa)	S_{eq} (Pa)	Design Life n	N^*	D^*
2	m^*	7.8794		1.037E+06	1.482E+08	1.56E+08	1.984E+03	1.054E+08	1.883E-05
3	e^*	-0.0036		1.021E+06	1.459E+08	1.54E+08	0.000E+00	1.193E+08	0.000E+00
4	$F.M^*$	0.9591		1.004E+06	1.434E+08	1.51E+08	1.144E+00	1.361E+08	8.405E-09
5	$X.m^*$	119338.9474		9.842E+05	1.406E+08	1.48E+08	0.000E+00	1.593E+08	0.000E+00
6	$S.o$	322000000		9.769E+05	1.396E+08	1.47E+08	1.436E+00	1.689E+08	8.503E-09
7	W	0.007		9.555E+05	1.365E+08	1.44E+08	6.977E-05	2.011E+08	3.469E-13
8	E	2.97E+10		9.461E+05	1.352E+08	1.43E+08	1.407E+00	2.174E+08	6.472E-09
9				9.406E+05	1.344E+08	1.42E+08	1.211E-06	2.276E+08	5.322E-15
10	Damage	0.0282		9.330E+05	1.333E+08	1.41E+08	4.643E+01	2.427E+08	1.913E-07

b. code

	A	B
1	$\log K^*$	-12.2978
2	m^*	7.8794
3	e^*	-0.00357808249627971
4	$F.M^*$	0.959127465299723
5	$X.m^*$	119338.947368421
6	$S.o$	322000000
7	W	0.007
8	E	29700000000
9		
10	Damage	=SUM(I2:I55)

	D	E	F	G	H	I
1	X (N-m)	S (Pa)	S_{eq} (Pa)	n	N^*	D^*
2	1037150	=D2/\$B\$7	=E2/(1-(\$B\$5/\$B\$7)/\$B\$6)	1984.4358	=10^(\$B\$1-\$B\$2*LOG(F2/(2*\$B\$8))+\$B\$3)	=G2/H2
3	1021000	=D3/\$B\$7	=E3/(1-(\$B\$5/\$B\$7)/\$B\$6)	0	=10^(\$B\$1-\$B\$2*LOG(F3/(2*\$B\$8))+\$B\$3)	=G3/H3
4	1004075	=D4/\$B\$7	=E4/(1-(\$B\$5/\$B\$7)/\$B\$6)	1.1436941	=10^(\$B\$1-\$B\$2*LOG(F4/(2*\$B\$8))+\$B\$3)	=G4/H4
5	984200	=D5/\$B\$7	=E5/(1-(\$B\$5/\$B\$7)/\$B\$6)	0	=10^(\$B\$1-\$B\$2*LOG(F5/(2*\$B\$8))+\$B\$3)	=G5/H5
6	976925	=D6/\$B\$7	=E6/(1-(\$B\$5/\$B\$7)/\$B\$6)	1.4360063	=10^(\$B\$1-\$B\$2*LOG(F6/(2*\$B\$8))+\$B\$3)	=G6/H6
7	955500	=D7/\$B\$7	=E7/(1-(\$B\$5/\$B\$7)/\$B\$6)	0.0000697	=10^(\$B\$1-\$B\$2*LOG(F7/(2*\$B\$8))+\$B\$3)	=G7/H7
8	946125	=D8/\$B\$7	=E8/(1-(\$B\$5/\$B\$7)/\$B\$6)	1.4068975	=10^(\$B\$1-\$B\$2*LOG(F8/(2*\$B\$8))+\$B\$3)	=G8/H8
9	940600	=D9/\$B\$7	=E9/(1-(\$B\$5/\$B\$7)/\$B\$6)	1.2114993	=10^(\$B\$1-\$B\$2*LOG(F9/(2*\$B\$8))+\$B\$3)	=G9/H9
10	933000	=D10/\$B\$7	=E10/(1-(\$B\$5/\$B\$7)/\$B\$6)	46.426540	=10^(\$B\$1-\$B\$2*LOG(F10/(2*\$B\$8))+\$B\$3)	=G10/H10

ii. Microsoft Excel code for first order reliability method (Table 5.4)

a. example

	A	B	C	D	E	F	G	H	I	J
1										
2	log K	-12.2978	0.4810	-11.7423	1.1548	1	-0.9956	0	0	0
3	m	7.8794	0.2286	7.6060	-1.1961	-0.9956	1	0	0	0
4	e	-0.004	0.398	-1.3491	-3.3849	0	0	1	0	0
5	F.M	0.959	0.155	1.0445	0.5498	0	0	0	1	0
6	X.m	119339	82573	119338.9474	0.0000	0	0	0	0	1
7										
8	S.o	3.22E+08				-4.097302	-5.275339	-3.38493	0.549827	0.000
9	E	2.97E+10								
10										
11		β	3.65				D(x)	0.9574		
12		P.f	1.30E-04				g(x)	0.0000		
13		W	0.007	m ³						

b. code

	A	B	C	D	E
1					
2	log K	-12.2978	0.481	-11.7423287912718	=(D2-B2)/C2
3	m	7.8794	0.2286	7.60597944517367	=(D3-B3)/C3
4	e	-0.00357808249627971	0.397512001092447	-1.34912687067818	=(D4-B4)/C4
5	F.M	0.959127465299723	0.155291051813944	1.04451073958523	=(D5-B5)/C5
6	X.m	119338.947368421	82573.4895126805	119338.947380702	=(D6-B6)/C6
7					
8	S.o	322000000			
9	E	29700000000			
10					
11		β	=SQRT(MMULT(F8:J8,E2:E6))		
12		P.f	=1-NORMSDIST(C11)		
13		W	0.007	m ³	

	F	G	H
1			
2	1	-0.9956	0
3	-0.9956	1	0
4	0	0	1
5	0	0	0
6	0	0	0
7			
8	=MMULT(TRANSPOSE(E2:E6),MINVERSE(F2:J6))		=MMULT(TRANSPOSE(E2:E6),MINVERSE(F2:J6))
9			
10			
11		D(x)	=SUM(F17:F70)
12		g(x)	=1-D5*H11

	I	J
1		
2	0	0
3	0	0
4	0	0
5	1	0
6	0	1
7		
8	=MMULT(TRANPOSE(E2:E6),MINVERSE(F2:J6))	=MMULT(TRANPOSE(E2:E6),MINVERSE(F2:J6))

	A	B	C	D	E	F	G	H	I	J
1										
2	log K	-12.2978	0.4810	-11.1						
3	m	7.8794	0.2286	7.6						
4	e	-0.004	0.398	-1.3						
5	F.M	0.959	0.155	1.0						
6	X.m	119339	82573	11933						
7										
8	S.o	3.22E+08								
9	E	2.97E+10								
10										
11		β	3.65							
12		P.f	1.30E-04							
13		W	0.007	m^3						
14										

Solver Parameters

Set Target Cell:

Equal To: ☐ Max ☒ Min ☐ Value of:

By Changing Cells:

Subject to the Constraints:

APPENDIX E

i. Microsoft Excel code for calibration of load factor γ_f (Table 6.1)

a. example

	A	B	C	D	E	F	G	H	I	J	K	L
1	W	0.006904		X	S	n	Δn	S.avg	S.eq	Design log N	N	D
2	E	2.97E+10		1100000	1.59E+08	1.46E+05	4.85E+03	1.59E+08	1.65E+08	6.66	4.56E+06	1.06E-03
3	N.r	7.36E+07		1097500	1.59E+08	1.51E+05	5.01E+03	1.59E+08	1.65E+08	6.67	4.64E+06	1.08E-03
4	X.c	939358		1095000	1.59E+08	1.56E+05	5.18E+03	1.58E+08	1.65E+08	6.67	4.73E+06	1.10E-03
5	k.R	1.409		1092500	1.58E+08	1.61E+05	5.35E+03	1.58E+08	1.64E+08	6.68	4.81E+06	1.11E-03
6	X.a	485750		1090000	1.58E+08	1.66E+05	5.53E+03	1.58E+08	1.64E+08	6.69	4.90E+06	1.13E-03
7	yf	1.111		1087500	1.58E+08	1.72E+05	5.71E+03	1.57E+08	1.63E+08	6.70	4.99E+06	1.14E-03
8	ym	1.162		1085000	1.57E+08	1.78E+05	5.90E+03	1.57E+08	1.63E+08	6.71	5.08E+06	1.16E-03
9	S.o	3.22E+08		1082500	1.57E+08	1.84E+05	6.10E+03	1.57E+08	1.63E+08	6.71	5.17E+06	1.18E-03
10	S.m	11933895		1080000	1.56E+08	1.90E+05	6.30E+03	1.56E+08	1.62E+08	6.72	5.27E+06	1.20E-03
11	log K	-12.2978		1077500	1.56E+08	1.96E+05	6.51E+03	1.56E+08	1.62E+08	6.73	5.37E+06	1.21E-03
12	m	7.8794		1075000	1.56E+08	2.03E+05	6.72E+03	1.56E+08	1.62E+08	6.74	5.46E+06	1.23E-03
13	σ_e	0.397512		1072500	1.55E+08	2.09E+05	6.95E+03	1.55E+08	1.61E+08	6.75	5.57E+06	1.25E-03
14				1070000	1.55E+08	2.16E+05	7.18E+03	1.55E+08	1.61E+08	6.75	5.67E+06	1.27E-03
15	Damage	1.00		1067500	1.55E+08	2.23E+05	7.42E+03	1.54E+08	1.60E+08	6.76	5.77E+06	1.28E-03

b. code

	A	B	C	D	E	F	G	H	I	J	K	L
1	W	0.006904										
2	E	2.97E+10										
3	N.r	7.36E+07										
4	X.c	939358										
5	k.R	1.409										
6	X.a	485750										
7	yf	1.111										
8	ym	1.162										
9	S.o	3.22E+08										
10	S.m	11933895										
11	log K	-12.2978										
12	m	7.8794										
13	σ_e	0.397512										
14												
15	Damage	1.00										
16				1065000	1.54E+08	2.31E+05	7.66E+03	1.54E+08	1.60E+08	6.77	5.88E+06	1.30E-03

	D	E	F	G
1	X	S	n	Δn
2	1100000	=D2/\$B\$1	=10^(LOG(3*\$B\$3)*(1-\$B\$1/(\$B\$5*\$B\$4)*(E2/\$B\$7-\$B\$6/\$B\$1)))	=F3-F2
3	1097500	=D3/\$B\$1	=10^(LOG(3*\$B\$3)*(1-\$B\$1/(\$B\$5*\$B\$4)*(E3/\$B\$7-\$B\$6/\$B\$1)))	=F4-F3
4	1095000	=D4/\$B\$1	=10^(LOG(3*\$B\$3)*(1-\$B\$1/(\$B\$5*\$B\$4)*(E4/\$B\$7-\$B\$6/\$B\$1)))	=F5-F4

	H	I	J	K	L
1	S.avg	S.eq	Design log N	N	D
2	=AVERAGE(E2:E3)	=H2/(1-\$B\$10/\$B\$9)	=(\$B\$11-\$B\$12*LOG(\$B\$8*H2/(2*\$B\$2)))-2*\$B\$13	=10^J2	=G2/K2
3	=AVERAGE(E3:E4)	=H3/(1-\$B\$10/\$B\$9)	=(\$B\$11-\$B\$12*LOG(\$B\$8*H3/(2*\$B\$2)))-2*\$B\$13	=10^J3	=G3/K3
4	=AVERAGE(E4:E5)	=H4/(1-\$B\$10/\$B\$9)	=(\$B\$11-\$B\$12*LOG(\$B\$8*H4/(2*\$B\$2)))-2*\$B\$13	=10^J4	=G4/K4

REFERENCES

- Ayyub, B., & McCuen, R. (1997). *Probability, Statistics, & Reliability for Engineers*. Boca Raton: CRC Press.
- Dowling, N. E. (2007). *Mechanical Behavior of Materials*. Upper Saddle River: Pearson.
- Echtermeyer, A. (1993). *Fatigue of composite structures - influence of matrix and fabric*. Det Norske Veritas.
- Echtermeyer, A. (1994). Fatigue of glass reinforced composites described by one standard fatigue lifetime curve. *European Wind Energy Conference*, (pp. 391-396). Thessaloniki, Greece.
- Hurley, S., & Arockiasamy, M. (2011). Reliability-based fatigue life estimation of ocean current turbine rotor blades. *ASME 2011 30th International Conference on Ocean, Offshore, and Arctic Engineering*. Rotterdam, The Netherlands: ASME.
- Ingeniørforening, D. (1992). *Code of Practice for loads and safety of wind turbine structures*. Copenhagen, Denmark: Dansk Ingeniørforening.
- Lalanne, C. (1999). *Mechanical Vibration & Shock, Fatigue Damage*. Taylor and Francis Books, Inc.
- N. Barltrop, K. V. (2006). Wave-current interactions in marine current turbines. *IMechE*, 195-203.
- Phoon, B. L. (2002). Practical first-order reliability computations using spreadsheet. *Probabilistics in Geotechnics: Technical and Economic Risk Estimation* (pp. 39-46). Graz, Australia: Verlag Gluckauf GmbH. Essen.
- Ronold, K. O., Wedel-Heinen, J., & Christensen, C. (1999). Reliability-based fatigue design of wind-turbine rotor blades. *Engineering Structures*, 1101-1114.

- Senat, J. and M. Arockiasamy (2011). *ASME 2011 30th International Conference on Ocean, Offshore, and Arctic Engineering*. Rotterdam, The Netherlands: ASME.
- Senat, J. (2011). Numerical simulation and prediction of loads in marine current turbine full-scale rotor blades. *Thesis* . Boca Raton, FL: Florida Atlantic University.
- Somers, D. (1997). *Design and experimental results for the S814 airfoil*. Golden, Colorado: NREL.
- Toft, H., & Sorensen, J. (2010). Partial Safety Factors for Fatigue Design of Wind Turbine Blades. Denmark: Aalborg University and Risø-DTU.